

## **New findings of *Stephanorhinus kirchbergensis* in Siberia**

**Y.V. Lobachev, A.V. Shpansky, A.A. Bondarev, A.Y. Lobachev, S.K. Vasiliev,  
A.M. Klementev, I.E. Grebnev, and V.I. Silaev**

### **ABSTRACT**

New findings of *Stephanorhinus kirchbergensis* (Jäger, 1839) remains, obtained from the Asian part of Russia, are described. The material includes 39 specimens from 13 localities in West Siberia and East Siberia. It considerably expands the geographic distribution of this species of rhinoceros. A series of 11 mandibles from Siberia, including one juvenile individual with deciduous teeth, is described for the first time. We also present a large set of data on well-preserved postcranial remains. The morphology and sizes of mandibles, teeth, and postcranial remains of adult individuals of *S. kirchbergensis* from Siberia are similar to individuals of this species described from European localities. A series of upper teeth was subjected to mesowear analysis to assess the diet of *S. kirchbergensis* from West Siberia. The chemical composition (including stable isotopes) of the Siberian *Stephanorhinus* teeth is analyzed for the first time. Comparisons of Siberian *S. kirchbergensis* with European *S. kirchbergensis* and West Siberian *Coelodonta antiquitatis* broaden our understanding of the ecology, variability, and evolution of *S. kirchbergensis* under climatic changes in continental settings from the Middle to the Late Pleistocene. Despite small samples, we can suppose that *S. kirchbergensis* was widely distributed in Siberia.

Y.V. Lobachev. PAO Novosibirsk Institute of Software Systems, Novosibirsk, Russia.  
yvlobachev@gmail.com

A.V. Shpansky. Tomsk State University, Russia. shpansky@ggf.tsu.ru

A.A. Bondarev. Omsk Regional Branch of the Russian Geographical Society, Omsk 644007, Russia.  
gilgamesh-lugal@mail.ru

A.Y. Lobachev. PAO Sberbank, Novosibirsk, Russia. inobges@gmail.com

S.K. Vasiliev. Institute of Archaeology and Ethnography of SB RAS, Russia. Svasiliev@archaeology.nsc.ru

A.M. Klementev. Institute of the Earth's Crust SB RAS, Russia. klem-al@bk.ru

I.E. Grebnev. Paleopark Altai Republic, Russia. mnh66@mail.ru

V.I. Silaev. Institute of Geology of Komi SC UB RAS, Syktyvkar, Russia, silaev@geo.komisc.ru

**Keywords:** *Stephanorhinus kirchbergensis*; bone morphology; Siberia; Middle Pleistocene; mesowear analysis

Lobachev, Y.V., Shpansky, A.V., Bondarev, A.A., Lobachev, A.Y., Vasiliev, S.K., Klementev, A.M., Grebnev, I.E., and Silaev, V.I. 2021. New findings of *Stephanorhinus kirchbergensis* in Siberia. *Palaeontologia Electronica*, 24(1):a14. <https://doi.org/10.26879/734>  
[palaeo-electronica.org/content/2021/3322-stephanorhinus-kirchbergensis-in-siberia](https://palaeo-electronica.org/content/2021/3322-stephanorhinus-kirchbergensis-in-siberia)

Copyright: April 2021 Palaeontological Association.

This is an open access article distributed under the terms of Attribution-NonCommercial-ShareAlike 4.0 International (CC BY-NC-SA 4.0), which permits users to copy and redistribute the material in any medium or format, provided it is not used for commercial purposes and the original author and source are credited, with indications if any changes are made.  
[creativecommons.org/licenses/by-nc-sa/4.0/](https://creativecommons.org/licenses/by-nc-sa/4.0/)

## INTRODUCTION

Remains of *Stephanorhinus kirchbergensis* (Jäger, 1839) are relatively rare. There are about 80 localities known, most of them being in the European part of the geographic distribution. Only a few remains of *S. kirchbergensis* have been described from the Yakutia (Sakha) Republic and the Irkutsk, Kemerovo, and Tomsk Provinces, Russia (Billia, 2007, 2008b, 2011a, 2011b). The only skull from Siberia lacks georeferenced data but presumably came from the Irkutsk Province (Chersky, 1874; Billia, 2008a). Dubrovo (1957) described *S. kirchbergensis* teeth (previously *Rhinoceros mercki*) and *Mammuthus trogontherii* remains (previously *Parelephas wüsti*) from the Vilyuy River (Yakutia). Isolated teeth of *S. kirchbergensis* were reported in Mohovsk Quarry and the Inya River of the Kemerovo Province (Billia, 2007). Most *S. kirchbergensis* remains from Russia, more than 30 teeth and bones, were found in Krasniy Yar (Tomsk Province) (Alekseeva, 1980; Shpansky and Billia, 2012; Shpansky, 2016). All of the previously described material from Siberia was assigned to the Middle Pleistocene (Volkova and Babushkin, 2000).

In the last few years, a large series of new findings of *Stephanorhinus kirchbergensis* was obtained from southern West Siberia, including the Altai and Krasnoyarsk Territories and the Novosibirsk, Omsk, Tomsk, and Irkutsk Provinces. The new material, described here for the first time, came from 13 localities in the southern part of West Siberia and East Siberia (Figure 1). The material consists of 39 samples, including a series of 11 mandibles. One mandible belongs to a juvenile with deciduous teeth. Most of the samples did not have a stratigraphic provenance as they were collected on riverbanks.

## MATERIAL

### Altai Territory

A collection of 5,806 bones, which were attributed to 24 species of mammals of the Middle and Late Pleistocene, was gathered on river beaches and shallows of the Chumysh River between the villages Martynovo and Kytmanovo since 2010. The most numerous remains were found near Novoduplenka village (53°27' N, 85°41'

E) (Figure 1). The findings near Novoduplenka include 19 very well-preserved specimens assigned to *Stephanorhinus kirchbergensis*: three mandibular corpora (including one belonging to a juvenile individual with deciduous teeth), one vertical mandibular ramus, eight upper teeth, and seven postcranial bones (Table 1) (Lobachev et al., 2014; Vasiliev et al., 2014).

In the study area, the Chumysh River exposed the deposits of low first and second fluvial terraces, which were from 12 to 20 m high. Radiocarbon dating of wood remains from the lowest part of five sections in the valley of the Chumysh River (Kytmanovo, Staroglushinka, Sorokino, Pogorelka, Shadrintsevo) indicate a Karginian age within 38–24 <sup>14</sup>C ka BP (Rusanov and Orlova, 2013). Thirteen bones collected on the beaches between Martynovo and Kytmanovo were sampled for radiocarbon dating (no bones of *Stephanorhinus kirchbergensis* were sampled for radiocarbon dating). Four dates presented in a report (Lobachev et al., 2012) and nine unpublished dates indicate the age of the sampled fossils ranges from 44.5 to 22.3 <sup>14</sup>C ka BP. Taphonomic observations of the specimens by one of us (AVS) indicate that all mandibles (both juvenile and adult) were slightly rounded, which could reflect redeposition from more ancient deposits of the Middle to Upper Pleistocene. On this part of the Chumysh River, localities with deposits that suggest an older age are known, including clam shells (SB RAS-425) from base layer 6 in the settlement of Kytmanov (Rusanov and Orlova, 2013).

Two mandibles and two postcranial bones were found on the sandy shoals in the vicinity of Biysk (the exact location is unknown) (Table 1). It is assumed that these remains were washed away from the base layer of high terraces of the Biya River (Rusanov and Orlova, 2013). These natural outcrops are known near the village Staraya Azhinka (the height of the terrace is 64 m), 60 km to the east of Biysk, where alluvial deposits of the Middle–Upper Pleistocene are exposed. Some bones collected from the middle height of the terrace did not contain collagen (SB RAS-4003). Another outcrop, a 50 m high terrace, is on the right bank of the Biya River, upstream from Stanitsa Bahtemiskaya village, 30 km east of Biysk.

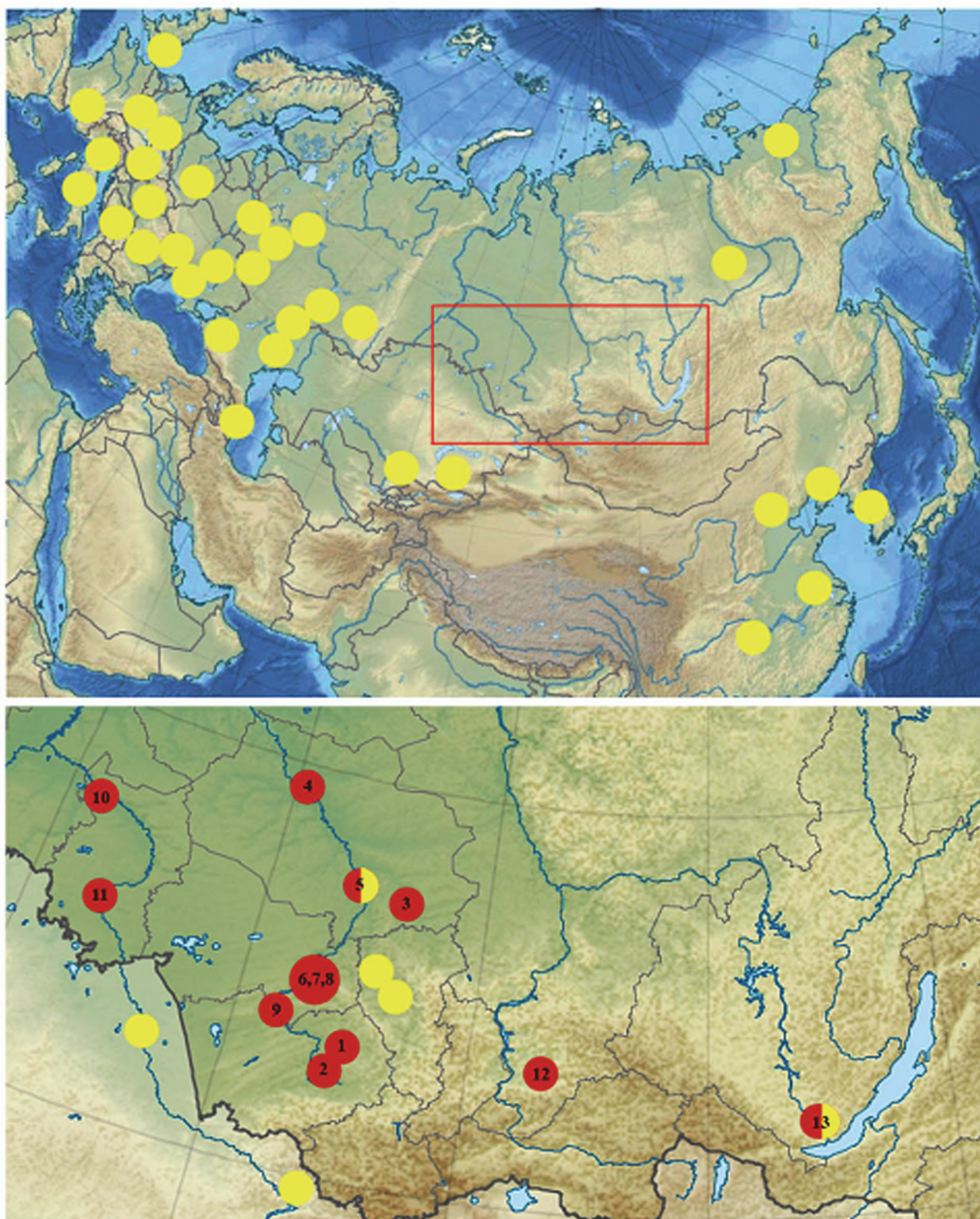


**FIGURE 1.** New findings of *Stephanorhinus kirchbergensis* remains in Western and Eastern Siberia. Red - new localities and finds, yellow - previously described localities. 1, Kytmanovo. 2, Biysk. 3, Asino. 4, Kindal. 5, Krasniy Yar, Tomsk Province. 6, Berdsk. 7, Krasniy Yar, Novosibirsk Province. 8, Bibiha. 9, Taradanovo. 10, Utuskun. 11, Omsk. 12, Kachulka. 13, Irkutsk Province.

### Tomsk Province

New remains from the Tomsk Province were found in the well-known locality Krasniy Yar (57°07' N, 84°30' E) (Alekseeva, 1980; Shpansky and Billa, 2012; Shpansky, 2016; Shpansky et al., 2016), as well as from Asino and Kindal (Figure 1). New findings comprise a mandibular corpus, an upper

tooth, and four postcranial bones (Table 1). The geological age is assumed to be Tobolian (MIS 11-9). The AMS radiocarbon analysis (UBA-21200 and UBA-21201) carried out on an astragalus of *Stephanorhinus kirchbergensis* (PM TSU 5/740) showed the absence of collagen in the bone (Shpansky et al., 2016).

**TABLE 1.** Material included in this study.

	<b>Locality</b>	<b>Skeletal element</b>	<b>Collection Name</b>
1	Kytmanovo, Chumysh River, Altay Territory	right M2	NSMML-1
		right P4	NSMML-2
		right M3	NSMML-3
		left M3	NSMML-4
		left M2	NSMML-5
		left P4	NSMML-6
		left P4	NSMML-7
		left P4	NSMML-8
		left metatarsal II	NSMML-101
		left metacarpal II	NSMML-102
		left metatarsal IV	NSMML-105
		astragalus	NSMML-107
		right radius	IAE CHU-108
		left ulna	NSMML-109
		conjoined left tibia and fibula	NSMML-110
		right body of mandible	NSMML-10
		left body of mandible, juvenile	NSMML-12
		right body of mandible	NSMML-26
		right ramus of mandible	NSMML-27
2	Biysk vicinity, Altay Territory	right body of mandible	GR PC-1164
		mandible	GR PC-1165
		left metacarpal II	GR PC-203
		right metacarpal II	GR PC-214
3	Asino, Chulym River, Tomsk Province	left M1	PM TSU 1/396
4	Kindal, Ob River, Tomsk Province	left body of mandible	KB MAN K-397
5	Krasniy Yar, Ob River, Tomsk Province	metacarpal III	PM TSU 5/5197
		Navicular	PM TSU 5/2538
		Navicular	PM TSU 5/3063
6	Berdsk vicinity Novosibirsk Province	third left upper molar M3	IAE BB-1
7	Krasniy Yar, Ob River, Novosibirsk Province	left body of mandible	NSMML 22090
		left body of mandible	IAE KY-4323
8	Bibiha, Ob River, Novosibirsk Province	right M2	NSMML 21052
9	Taradanovo, Ob River, Novosibirsk Province	left metacarpal IV	IAE TRD-17
		left metacarpal IV	IAE TRD-18
		left metatarsal IV	IAE TRD-2
10	Utuskun, Irtysh River, Omsk Province	right body of mandible	Sk_ui1
11	Omsk, Irtysh River, Omsk Province	left p4	Sk_oms1
12	Kachulka, Krasnoyarsk Territory	left p3	PM TSU № 1/395
13	Irkutsk Province	mandible	IRM 2436

A tooth (PM TSU 1/396) was found at a 8 m-depth in Tobolian deposits in a sand quarry east of Asino on the left bank of the Chulym River (57°04'N, 86°10'E).

The most remarkable specimen is a mandible (KB MAN K-397) found at 14 m below water level at the mouth of the Kindal oxbow, left bank of the Ob River, downstream from the Kargasok settlement in July 2011 by the local resident A.V. Bary-

shev. The locality is 400 km north of the city of Tomsk (Kargasok area of the Tomsk Province). The Kindal location of *Stephanorhinus kirchbergensis* is 59°08' N, 80°35'E, which is closer in latitude to the finding on the Vilyuy River in Yakutia (63°40' N) (Dubrovo, 1957).

### **Novosibirsk Province**

Mandibular corpora of two individuals of *Stephanorhinus kirchbergensis* (NSMLL 22090 and IAE KY-4323) were discovered in the Krasniy Yar locality (55°13' N, 82°52' E) on the left bank of the Ob River, 17 km north of the city of Novosibirsk (Figure 1). These remains were found among 3,336 bones of other species of large mammals that had inhabited the southeastern area of West Siberia in the Middle–Late Pleistocene. Samples were collected on the sandbank. Some of them wear marks of redeposition. Analysis of spores and pollen, seeds, ostracods, and mollusks revealed warm interglacial conditions at the time of layer deposition. Kazantsevo Horizon (MIS 5) is the most probable origin for the alluvial deposits of the channel of layer 6 (Martynov et al., 1977; Volkov and Arhipov, 1978; Panychev, 1979). A high proportion of the remains from this locality may have been redeposited, which suggests a considerable range in age. Thus, Middle Pleistocene age for *S. kirchbergensis* remains should not be excluded.

An upper molar (NSMLL 21052) was found near Bibiha village (55°19' N, 82°52' E) on the right bank of the Ob River, 26 km north of Novosibirsk (Table 1). This locality is represented by cross-bedded sands of the outcrop of the third fluvial terrace sloping below the water surface, similar to those at Krasniy Yar (Novosibirsk Province), layer 6.

An upper left molar (IAE BB-1) was found during dredger activities within the city limits of Berdsk (Table 1). The exact location is unknown.

Three rhinoceros metapodials were discovered among the numerous large mammalian remains from Taradanovo (53°48'N, 81°49'E) on the Ob River (Suzun area of the Novosibirsk Province) (Figure 1, Table 1). All megafaunal remains are redeposited. The main bone-bearing horizon of the Taradanovsk highbank is located several meters below the lowest shore line. The section of highbank near Taradanovo has a similar structure to that at Krasniy Yar near Novosibirsk. Eighteen radiocarbon datings were obtained from the bones collected from the beach: 13 dates indicate an age older than 45–40 14C ka BP, which is close to the limits of the method, and five dates indicate an age of 36–26 14C ka BP (Vasiliev and Orlova, 2006).

The diversity of fauna includes the species of the beginning of Late Pleistocene, which allows estimating its geological age. One of us (SKV) thus supposes that the main bone-bearing layer in Taradanovo was formed during the Kazantsevoian (MIS 5).

### **Omsk Province**

A mandibular corpus (Sk\_ui1) was found by local historian N. B. Peristov in the Irtys River near Krasnoyarka and Utuskun villages of the Ust-Ishymsk district, Omsk Province (57°44'N, 71°17'E) (Figure 1). The Ust-Ishymsk area includes a group of early–Late Pleistocene mammal-bearing localities, typical for the area of latitudinal flow of the Irtys River. Terrace deposits of Karginian and Sartaian ages are located in the vicinity of the site (Krivonogov, 1988). Up and down the stream of the Irtys River, the outcrops of lower and Middle Pleistocene are exposed on the right bank. Lower Pleistocene sediments are observed in the outcrops of the upland “Tobolsk continent”: the Koltyrminsk, Narimanovsk, Nikolsk, Romanovsk, and Sakanairsk cliffs.

A lower fourth premolar (Sk\_oms1) was found by local historian A. L. Dorogov in Omsk on the bank of the Irtys River. A lithological description of natural outcrops of the valley became impossible due to anthropogenic activities. Mammal bones of various ages from the Pliocene to the present occur within the city on the sandbanks and in artificial outcrops.

### **Krasnoyarsk Territory**

A lower third premolar (PM TSU 1/395) was found in Kachulka village (53°47'N, 92°54'E), Karatuzsk district, Krasnoyarsk Territory, 100 km east of Minusinsk at the confluence of the Amyl and Kazyr rivers (Figure 1, Table 1). The tooth was buried in fine-grained sands at a depth of about 3 m. Its preservation suggests redeposition from older deposits. This finding in the south of the Krasnoyarsk Territory is the first in this region and an important link between West Siberia and East Siberia in the geographic distribution of *S. kirchbergensis*.

### **Irkutsk Province**

A cranium and a mandible are known. The locality for a mandible (IRM 2436) stored in the Irkutsk local history museum (Table 1) is unknown. It may belong to the same individual as a cranium (ZIN 10718; Chersky, 1874), but the locality for the cranium is also undefined.

### Institutional Abbreviations

IAE CHU: Institute of Archaeology and Ethnography, Siberian Branch, Novosibirsk, collection from Chumysh; IAE KY: Institute of Archaeology and Ethnography, Siberian Branch, Novosibirsk, collection from Krasniy Yar (Novosibirsk Province); IAE TRD: Institute of Archaeology and Ethnography, Siberian Branch, Novosibirsk, collection from Tara-danovo; IAE BB: Institute of Archaeology and Ethnography, Siberian Branch, Novosibirsk, collection from Biysk; NSMLL: Novosibirsk State Museum of Local Lore, Novosibirsk; IRM: Irkutsk Regional Museum, Irkutsk; TRM: Tomsk Regional Museum, Tomsk; KB MAN K: Kargasok branch of the Museum of Art of the North, Kargasok, Tomsk Province; PM TSU: Paleontological Museum of Tomsk State University, Tomsk; Sk\_oms1: Omsk Province, the Bondarev private collection; Sk\_ui1: Omsk, the Bondarev private collection; GR PC: The I. Grebnev private collection.

### METHODS

#### Morphometrics

Descriptions of morphological and morphometric features of teeth and measurements of mandibles and postcranial bones were made following Gromova (1935), Guérin (1980), Lacombe (2005, 2006), Kahlke (1977), Fortelius (1982), Clauss et al. (2008), Dubrovo (1957), and Fortelius et al. (1993).

The following dimensions were used for morphometric analysis of rhinoceros mandibles:

- 1) overall length of mandible;
- 2) length from the mesial edge of the p2 alveoli to the distal edge of the vertical ramus;
- 3) alveolar length of dentition p2-m3 (AL);
- 4) alveolar length of premolar row p2-p4;
- 5) alveolar length of molar row m1-m3 (ALm1\_m3);
- 6) height of mandibular corpus between p2 and p3 (HMB\_p3);
- 7) height of mandibular corpus between p3 and p4 (HMB\_p4);
- 8) height of mandibular corpus between p4 and m1 (HMB\_m1);
- 9) height of mandibular corpus between m1 and m2 (HMB\_m2);
- 10) height of mandibular corpus between m2 and m3 (HMB\_m3);
- 11) transverse diameter of mandibular corpus between p2 and p3 (TMB\_p3);

- 12) transverse diameter of mandibular corpus between p3 and p4 (TMB\_p4);
- 13) transverse diameter of mandibular corpus between p4 and m1 (TMB\_m1);
- 14) transverse diameter of mandibular corpus between m1 and m2 (TMB\_m2);
- 15) transverse diameter of mandibular corpus between m2 and m3 (TMB\_m3);
- 16) length of mandibular symphysis;
- 17) length of diastema;
- 18) width of incisal area of the symphysis;
- 19) thickness of the symphysis distally;
- 20) transverse diameter of mandibular condyle;
- 21) height of mandibular condyle;
- 22) height from the level of the occlusal surface of dentition to the mandibular condyle;
- 23) distance from the level of the mandibular condyle to the distal edge of the m3 alveoli; and
- 24) height of mandibular corpus before p2 (HMB\_p2).

The following indices were used for comparative analysis of *Stephanorhinus kirchbergensis* and *Coelodonta antiquitatis* mandibles: index 1 =  $ALm1\_m3 / AL$ ; index 2 =  $HMB\_p2 / AL$ ; index 3 =  $HMB\_p3 / AL$ ; index 4 =  $HMB\_p4 / AL$ ; index 5 =  $HMB\_m1 / AL$ ; index 6 =  $HMB\_m2 / AL$ ; index 7 =  $HMB\_m3 / AL$ ; index 8 =  $TMB\_p3 / AL$ ; index 9 =  $TMB\_p4 / AL$ ; index 10 =  $TMB\_m1 / AL$ ; index 11 =  $TMB\_m2 / AL$ ; index 12 =  $TMB\_m3 / AL$ .

The biological age of an individual animal was determined based on the mandible by using the method introduced by Hitchins (1978) and Hillman-Smith et al. (1986). First, several stages reflecting the degree of tooth development and wear were identified.

The stages for upper teeth (STU) are:

- 1) presence of a dentine nucleus in the alveolus (STU1);
- 2) dental crown erupted over the bone tissue but unworn (STU2);
- 3) apices of most protruding cusps slightly worn (STU3);
- 4) apices of most protruding cusps worn, but wear does not affect steep ridges (STU4);
- 5) dental crown more worn than STU4, occlusal surface has continuous sections (STU5);
- 6) dental crown worn by at least 50%, occlusal part smooth, median valley still open (STU6);
- 7) dental crown worn more than 50%, median valley closed (STU7);

- 8) dental crown heavily worn, the median valley closed by dentine on every side (STU8);
- 9) presence of few remains of enamel, fragmentary mesial and distal valleys (median valley disappeared) (STU9); and
- 10) absence of enamel, crown totally worn (STU10).

The stages for lower teeth (STL) are:

- 1) erupting below the bone surface (STL1);
- 2) erupting above but unworn (STL2);
- 3) very slight wear, tips of cusps shiny (STL3);
- 4) slight wear exposing dentine on cusps, but ridges steep with deep gaps (STL4);
- 5) more wear than STL4, but still with deep gaps (STL5);
- 6) medium wear, tooth surface becoming fairly flat, but infundibulum channel still open (STL6);
- 7) medium/heavy wear, channel just closed (STL7);
- 8) heavy wear, channel fully closed, through dentine (STL8);
- 9) very heavy wear, small patches of enamel remaining (STL9); and
- 10) no enamel remaining (STL10).

It is assumed that each tooth at each moment of its biological age corresponded to one of the above stages. Thus, the individual age of the animal could be defined by the cumulative information on each tooth stage from the jaw tested, comparing it to the stages given in the tables by Hillman-Smith et al. (1986).

The following measurements were used to analyze postcranial bones of rhinoceroses:

- 1) maximum length in the sagittal plane (ML);
- 2) antero-posterior diameter of the proximal epiphysis (APD);
- 3) transverse diameter of the proximal epiphysis (TD);
- 4) antero-posterior diameter of the distal epiphysis (APDde);
- 5) transverse diameter of the distal epiphysis (TDde);
- 6) transverse diameter of the distal joint (TDdj);
- 7) transverse diameter of the diaphysis in the middle (mTDd);
- 8) antero-posterior diameter of the diaphysis in the middle (mAPDd);
- 9) transverse diameter of the tuberositas tibia (TDtt);

- 10) maximum transverse diameter measured perpendicularly to the vertical axis of the astragalus (ATD);
- 11) maximum height, measured perpendicularly to the first diameter of the astragalus (AH);
- 12) transverse diameter of distal joint of the astragalus (ATD artic. dist.);
- 13) transverse diameter of distal part of the astragalus below the collar (ATD max dist.);
- 14) transverse diameter of the olecranon (TD olecr.);
- 15) antero-posterior diameter of the olecranon (APD olecr.);
- 16) transverse diameter of the proximal joint (TD artic. prox.); and
- 17) maximum height of the proximal joint (H artic. prox.).

### Mesowear Analysis

The mesowear method developed by Fortelius and Solounias (2000) was applied to reconstruct the dietary preferences of *Stephanorhinus kirchbergensis* and *Coelodonta antiquitatis* in the southeast area of West Siberia. The method is based on the study of facet development on the buccal side of occlusal surfaces of upper molar M2 of ungulates. The main factor in the formation of facets in the area of the paracone and metacone is the close interaction of the upper and lower teeth during mastication (attrition). The other factor that affects the formation of the occlusal surface is the mechanical properties of the food items that crushed by the teeth. Consuming rough and abrasive food leads to smoothing of the wear surface of the cusps by contact with each other. Mesowear analysis deals with three variables: hypsodonty index, wear surface relief (l, low; h, high), and the shape of cusps (s, sharp; r, rounded; b, blunt). A conservative approach was used to select the paracone or metacone cusp (Fortelius and Solounias, 2000), i.e., the sharpest one. The cusp was considered high if the proportion of its height to the crown width was larger than 0.03, which was the empirical definition for rhinoceroses (Fortelius and Solounias, 2000). Teeth in the first and last dental wear stages were not considered in the analysis. The method was applied for teeth in stages STU5 to STU8. A data set of more than 20 specimens is considered statistically significant, while a set of more than 10 individuals allows seeing the main vector of the adaptation process toward one or another dietary preference.

The mesowear method was extended by Kaiser and Solounias (2003) where not only M2 but all possible combinations of upper teeth were used in investigations of diet signals. In particular, the research showed that statistical data obtained from the set of four teeth P4–M3 were sufficiently close to those that were obtained while using only M2. Thus, limited fossil material can be used by applying mesowear analysis to the set consisting of P4–M3.

Ten upper teeth of *Stephanorhinus kirchbergensis* presented in this article and two upper P4 and M1 from the Tomsk Province presented by Shpansky and Billia (2012) were used as material for mesowear analysis.

Statistical analysis was carried out using Statistical Package for the Social Sciences (SPSS) version 21 and Sysstat version 12. Because the independent samples of *Stephanorhinus kirchbergensis* and *Coelodonta antiquitatis* investigated were not normally distributed, the nonparametric Mann-Whitney U-test (SPSS 21) was used to determine the degrees of difference of their mesowear signals. Hierarchical cluster analysis with complete linkage in a mode (the farthest neighbor, with interval measure) of Euclidean distance was applied following the standard hierarchical amalgamation method. As an input for cluster analysis, the percentages of independent mesowear signals were used: the percentage of high relief, the percentage of sharp peaks, and the percentage of blunt peaks. Mesowear signals of *C. antiquitatis* teeth from southern localities of West Siberia from the collection of IAE were used as a reference material. Data from subgroups of 27 typical recent animals presented in Fortelius and Solounias (2000) were also used. Reference material on *Stephanorhinus* was taken from Kahlke and Kaiser (2011) and van Asperen and Kahlke (2014). A conservative model of dietary classification was used in classifying the animals by their dietary preferences (Fortelius and Solounias, 2000).

### Biogeochemistry

The study was conducted as part of an interdisciplinary research project on the study of bone detritus of Cenozoic vertebrata in the Institute of Geology, Komi Science Centre, Project Manager V. I. Silaev. Analysis of the chemical and stable isotopic composition was conducted using a broad set of methods including several types of spectroscopy and mass spectrometry. Methodological approaches are described in more detail in a separate paper (Silaev et al., 2015).

## DESCRIPTION

Material of *Stephanorhinus kirchbergensis* from 13 localities, consisting of 39 samples, is described (Table 1). Published materials on the European *S. kirchbergensis* and *Coelodonta antiquitatis* were taken as the comparison.

### Mandibles

Specimen NSMLL-12 (Figure 2, Table 2) is a fragment of left mandibular corpus of a juvenile individual. The rostral part is broken on the level of symphysis, while the caudal part is absent behind the alveolus for m1. The symphysis area shows gnaw marks from small animals. The jaw is relatively low; the width of the corpus gradually increases from dp1 toward dp4. Widening of the ventral part of the corpus is not visible. The mandible has an oval shape in the transverse plane, while it is pear-shaped in *Coelodonta antiquitatis*. Teeth dp2–4 are present. The metalophid of dp2 is slightly worn, and the hypolophid is worn by 5–10% (STL5); metalophid and hypolophid in dp3 are worn for approximately 5–10% (STL5); dp4 is on the fourth stage of wear (STL4). Alveolar length of the tooth row dp1–dp4 is 138 mm. dp1 is absent. Its alveolus is well developed and round. The alveolar cavity for m1 is large. The edges of the alveolus are directed toward each other, which shows the initial stage of tooth eruption (formation of the crown is at the first stage, STL1). The enamel is smooth, without a clear pattern of enamel prisms. The paraconid is absent in dp2. A fold-like undeveloped third valley near the parastylid is present on dp3. The main valleys on dp2, dp3, and dp4 are broad and U-shaped. Mesiodistal compression of the crowns is not seen. Deciduous crowns have a vertically convex shape on the buccal side. The valley between lophids is deep. Lophids are convex in occlusal view. In the first phase of the chewing process, a browser forms the facets on the buccal side of the lower teeth at an acute angle to the occlusal surface. On the teeth of the given mandible, these facets are in the initial stage of forming. The underdeveloped folds of cingulid are present on the lingual side of dp4 and in dp2–dp4 on the buccal side in the ventral part of the metalophid. Cementum is absent. The estimated biological age of the individual is less than two years.

All of the mandibles listed below for adult individuals show the following features. The mandibular corpus is relatively low. Its changes in height and transversal diameter from p2 to m3 are linear; the transverse section of the mandibular body is oval, without ventral extension. Teeth are large with



**FIGURE 2.** *Stephanorhinus kirchbergensis*; Chumysh River at Kytmanovo (Kytmanovo District, Altay Territory, southeast Western Siberia); the horizontal left body of a mandible of a juvenile rhino NSMML-12, occlusal and buccal views. Scale bar ruled in centimeters.



**FIGURE 3.** *Stephanorhinus kirchbergensis*; Chumysh River at Kytmanovo (Kytmanovo District, Altay Territory, southeast Western Siberia); the horizontal right body of a mandible NSMML-10, occlusal and buccal views. Scale bar ruled in centimeters.

smooth enamel, without a clear pattern of enamel prisms. All crowns are vertically convex and barrel-shaped on the buccal side. The valley between the lophids is distinct. The lophids of p3–m3 have a convex surface in occlusal view. On the lower teeth, there are facets on the buccal side at an acute angle to the occlusal surface. These facets were formed on the first phase of the browser's chewing process.

Specimen NSMML-10 (Figure 3, Tables 3, 4) is a fragment of mandible, the right mandibular body of an adult individual. The symphysis is preserved but is much damaged. The incisor edge of the symphysis is narrow, its dorsal surface is spoon-shaped, and the ventral surface is convex. The alveoli of the incisors are absent on the rostral edge of the symphysis. The caudal edge of the symphysis is on the level of p3, and the bone of the mandible at the caudal side of the symphysis is very thick. The left mandibular body is broken

between the alveoli of p3 and p4. The alveoli of p2 and p3 contain roots, but the crowns are destroyed. The right mandibular corpus is preserved together with the angular area, while the vertical ramus is broken off. The right dentary row p2–m3 is completely preserved. The diastema is relatively short. Dentition is highly worn: p2 (STL9), p3 (STL9), p4 (STL8), m1 (STL8), m2 (STL7), and m3 (STL6). The valleys are V-, or U-shaped and preserved only on m2 and m3. In p2–m2, there is a poorly developed cingulid on the buccal side of the ventral part of the metalophid and on the lingual side of the paraconid. Remains of a very thin layer of cementum are preserved on the back wall of m2 on the root area of the crown. A considerable level of wear suggests a biological age of the animal close to 30 years.

Specimen NSMML 22090 (Figure 4, Tables 3, 4) is fragment of mandible, the left mandibular corpus of an adult individual. The rostral part is broken

**TABLE 2.** metric comparison of lower deciduous teeth of *stephanorhinus kirchbergensis* and *coelodonta antiquitatis* of the middle and upper pleistocene from the altay territory and novosibirsk and tomsk provinces in southeastern western siberia versus european and chinese regions. all measurements are in mm. sample sizes are given in parentheses. Available in zipped download at <https://palaeo-electronica.org/content/2021/3322-stephanorhinus-kirchbergensis-in-siberia>.

**TABLE 3.** Metric comparison of lower permanent teeth of *Stephanorhinus kirchbergensis* and *Coelodonta antiquitatis* of the Middle and Upper Pleistocene from the Altay Territory and Novosibirsk and Tomsk Provinces in southeastern Western Siberia versus European and Chinese areas. All measurements are in mm. Sample sizes are given in parentheses. Available in zipped download at <https://palaeo-electronica.org/content/2021/3322-stephanorhinus-kirchbergensis-in-siberia>.

**TABLE 4.** Metric comparison of the mandibles of *Stephanorhinus kirchbergensis* and *Coelodonta antiquitatis* of the Middle and Upper Pleistocene from the Altay Territory and Novosibirsk, Tomsk, Omsk, and Irkutsk Provinces of southeastern Western Siberia versus European and Chinese areas. All measurements are in mm. Sample sizes are given in parentheses. Available in zipped download at <https://palaeo-electronica.org/content/2021/3322-stephanorhinus-kirchbergensis-in-siberia>.



**FIGURE 4.** *Stephanorhinus kirchbergensis*; Ob River at Krasniy Yar (Novosibirsk Province, southeast Western Siberia); the horizontal left body of a mandible NSMLL 22090, occlusal and buccal views. Scale bar ruled in centimeters.

near the p2, while the caudal end is lacking the portion behind the alveolus of m3. All teeth are present in the jaw from p2 to m3. They have an average stage of wear: p2 (STL7), p3 (STL7), p4 (STL6), m1 (STL7) m2 (STL6), and m3 (STL4). The trigonid basin of p4, m1, and m2 is wide and V-shaped. The mesial and distal valleys of m3 are wide and U-shaped. A poorly developed cingulid is present on the buccal side of the ventral part metalophid in p4, m2, and m3, and on the lingual side from the paraconid to the metaconid in p2–m2. Cementum is absent. The individual's estimated biological age is 16–20 years.

Specimen IAE KY-4323 (Figure 5, Tables 3, 4) is a fragment of mandible, the left mandibular corpus of an adult individual. The rostral part is broken



**FIGURE 5.** *Stephanorhinus kirchbergensis*; Ob River at Krasniy Yar (Novosibirsk Province, southeast Western Siberia); the horizontal left body of a mandible IAE KY-4323, occlusal and buccal views. Scale bar ruled in centimeters.



**FIGURE 6.** *Stephanorhinus kirchbergensis*; Omsk (Omsk Province, southeast Western Siberia); the horizontal right body of a mandible Sk\_ui1, occlusal and buccal views. Scale bar ruled in centimeters.

near p2. The caudal part is broken in the angular area. All teeth p2–m3 are present in the jaw but heavily worn: p2 (STL9), p3 (STL9), p4 (STL9), m1 (STL9), m2 (STL8), and m3 (STL7). The trigonid basin of m3 is U-shaped. The cingulid is present on p2–m2 on the buccal side of the ventral part of the metalophid and on the lingual side of the paraconid towards the metaconid. The cementum is not preserved. This is the smallest of all specimens presented in this overview, which may be correlated with sexual dimorphism and suggest an identification as a female individual. The estimated biological age of the individual is more than 30 years.

Specimen Sk\_ui1 (Figure 6, Tables 3, 4), is a fragment of a mandible, the right mandibular corpus of an adult individual. The specimen is broken off near the front edge of the p2 alveolus and the back edge of the m3 alveolus. The symphysis is partially preserved and is high and long, with an abrupt caudal edge at the middle part of p3. The tooth row from p3 to m3 is preserved in the jaw and shows average stages of wear: p3 (STL7), p4 (STL6), m1 (STL7), m2 (STL6), and m3 (STL4). The trigonid basin of m2 is V-shaped. Both valleys of m3 are wide and U-shaped. Folds of the cingulum are observed in the basal part of m2 and m3 crowns on the buccal side of the hypolophid and on the metalophids of p3 and p4. Signs of a thin layer of cementum are preserved on m1–m3. The estimated age of the individual is 20–25 years.

Specimen GR PC 1164 (Figure 7, Tables 3, 4) is a fragment of mandible, right horizontal mandibular corpus of adult individual. The symphysis is broken off near the alveolus of p2. The coronoid



**FIGURE 7.** *Stephanorhinus kirchbergensis*; Biysk (Altay Territory, southeast Western Siberia); the horizontal right body of a mandible GR PC-1164, occlusal and buccal views. Scale bar ruled in centimeters.

process is broken off from the vertical ramus. The mandibular condyle is broken from the lateral side. The mandibular corpus is very low compared to the other specimens. The notch of the symphysis is placed on the level of p3. The vertical ramus is relatively broad with a strongly developed masseteric fossa. The angle between the vertical ramus and the body is close to 90°. The mandibular body preserves p3–m1 but crowns are damaged. The crowns of p3 and p4 are worn to the level of the bottom of the mesial valley (STL7). Distal valleys are V-shaped. The m1 is worn to the level of the bottom of the distal valley (STL8). The signs of cingulid are observed on p3 on the lophid buccal side, and on the lingual side on p4 and m1. The distal edge of the m3 alveolus is close to the base of the vertical ramus. The area behind the m3 alveolus is wide and flat, with rounded edges. The estimated biological age of the individual is 20–25 years.

Specimen GR PC 1165 (Figure 8, Tables 3, 4) is the well-preserved mandible of adult individual. There is some damage to the right p2 alveolus and right coronoid process. The incisors' alveoli are absent. The left m1 (STL9) and m2 (STL8) are preserved but significantly damaged; the rest of the dentition is broken or missing. The right dentition is preserved, showing the high degree of wear: p4 (STL8), m1 (STL9), and m2 (STL8). Well-developed p2 alveoli show that there was no natural loss and overgrowth of alveoli in this specimen. The diastema is short. The notch of symphysis is placed on the level of p3, the bone of mandible at



**FIGURE 8.** *Stephanorhinus kirchbergensis*; Biysk (Altay Territory, southeast Western Siberia); the mandible GR PC-1165, 1, occlusal view. 2, posterior view. 3, buccal view. Scale bar ruled in centimeters.

the caudal extremity of symphysis is very thick. The symphysis is long and narrow, while the diastema is relatively short. Its dorsal surface is spoon-shaped. Its ventral surface is convex. The dorsal area behind the m3 is wide and flat with rounded edges. The vertical ramus of the mandible is relatively wide with strongly developed masseteric fossa. The angle between the vertical ramus and corpus is close to 90°. The left coronoid process is directed upwards; its tip does not bend in the caudal direction, as in *Coelodonta antiquitatis*. The condyles are very wide with a visible asymmetry in lateral direction. The medial edge of the condyle has a clear rectangular shape in caudal view. The lateral edge of the caudal part of the area posterior to the condyle process rises in a smooth, concave curve towards the condyle. In *C. antiquitatis*, this edge approaching the condyle becomes rounded towards the vertical axis of the vertical ramus of the mandible and becomes convex. The estimated biological age of the individual is 25–30 years.

Specimen IRM 2436 (Figure 9, Table 4) is a mandible of an adult individual with broken symphysis and coronoid processes. The notch of symphysis is placed at the level of p3, the bone at the



**FIGURE 9.** *Stephanorhinus kirchbergensis*; Irkutsk Province (southwest Eastern Siberia); a mandible IRM 2436, occlusal and buccal views. Scale bar ruled in centimeters.

caudal side of symphysis is very thick. The dorsal area behind the m3 is wide and flat with rounded edges. The mandibular body is relatively low. Its changes in height and transversal diameter from p2 to m3 are linear. The transverse section of the corpus is oval, without ventral extension. The vertical ramus is relatively broad with a strongly developed masseteric fossa. The angle between the vertical ramus and horizontal body is close to 90°. The condyles are very wide with a visible lateral asymmetry. The dentition is partly absent; the rest of it is broken. The paraconid, parastylid, and metaconid are broken on the left p4. The enamel is mostly absent; therefore the presence of cingulid is unclear. Mesial and distal valleys are shallow (depth of the distal valley is 7.0 mm). The thickness of the enamel on the hypoconid is 2.0 mm on the buccal side, 1.4 mm on the medial side. The metaconid is slightly worn. The estimated age of the individual is 20–25 years.

Specimen KB MAN K-397 (Figure 10.3-10.5, Tables 3, 4) is a fragment of mandible, left mandibular corpus of an adult individual, whose biological age is estimated to 15–17 years. The p3-m3 teeth

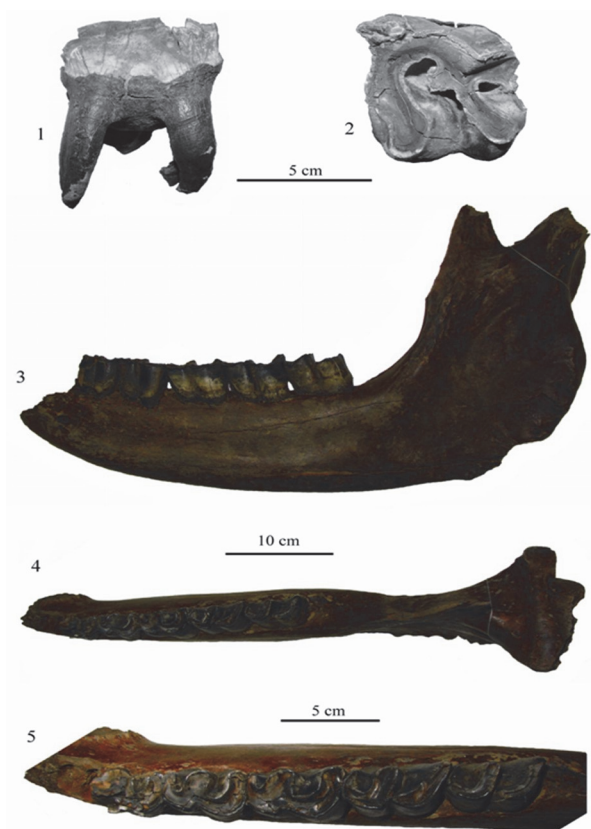


**FIGURE 10.** *Stephanorhinus kirchbergensis*; Tobol Horizon level (Middle Pleistocene); at Asino (Asino District, Tomsk Province, southeast Western Siberia); first left upper molar M1 PM TSU 1/396, 1. buccal view, 2. occlusal view. KB MAN K-397 the horizontal left body of a mandible of the Tobol Horizon level (Middle Pleistocene); Ob River at Kindal village (Kargasok District, Tomsk Province, southeast Western Siberia). 3, buccal view, 4, occlusal view, 5, occlusal view p3 – m3.

are preserved in the jaw. The caudal edge of the symphysis is on the same level as the middle part of p3, similarly to the condition seen in the specimen from Cherniy Yar (Gromova, 1935). The ventral edge of the mandibular body is almost smooth. The rise of the ventral edge is gradual from m1 to the symphysis, with increasing roundness in the symphysis area. Ventral margin is not concave in *Stephanorhinus kirchbergensis*. The thickness of the mandibular body is nearly the same along the whole tooth row, slightly decreasing under p3-p4. In transverse section, the mandibular corpus is high and oval-shaped, while it is pear-shaped with a ventral bulge in adult *Coelodonta antiquitatis*. Mental foramina (one large and several small) are placed under the p2 alveolus. The vertical ramus is relatively wide, with well-developed rugosity in the

angular area. The dorsal surface of the mandibular body behind the m3 is wide (62 mm), flattened, with a small longitudinal groove; the edges of the area are not sharp, as mentioned by Gromova (1935), and gently rounded, and the ridges are not developed. Its back surface forms an area that is broad and slightly concave in lateral view, perpendicular to the longitudinal axis of the jaw. In woolly rhinoceros, this area is considerably smaller, triangular, and oriented by a significant angle to the longitudinal axis. The articular head is inclined relative to the horizontal plane. Its medial edge is absent, and the lateral one is raised. Teeth crowns are high. The m3 is in the first stage of wear. Premolars are placed vertically to the alveolar edge of the mandibular body. Molars are significantly inclined forwards (Figure 10.3). Teeth are large, especially m1. Metrically, they are close to the samples from Moldavia, Povolzhy, and Taubach, but smaller than teeth from Krasniy Yar (Tomsk region). The length of the molar row m1–3 is 171 mm, which is larger than that in European samples. The closest length is in a large sample from Taubach (157.8–169.9 mm; Kahlke, 1977). Jaws from Chumysh River (NSMLL-10) and Krasniy Yar (Novosibirsk Province; NSMLL 22090) (Table 4) show similar dental size. The buccal cingulid is well defined on all metalophids and hypolophids of m1 and m2. The lingual cingulid is well developed on the metalophids of m1 and m2, and on the base of m3. The crown width near the roots is larger than on the apex, because of the slight inclination of the buccal surface. It is especially well observed on the slightly worn m2 and m3. In *C. antiquitatis*, the crown width is constant along the height. In this specimen of *S. kirchbergensis*, the metalophid on the molars is shorter than the hypolophid. The walls of lophids expand greatly to the base, forming valleys highly narrowed sharply downward. Metaconids are tapered roundly (without bulbosities) and are slightly abducted backwards on the protoconids of m2 and m3. The cementum fragments are preserved in the basal part. The enamel is smooth. There is a fusion of metalophid and hypolophid in p3–m1, the valleys are considerably deep. The fusion of metalophid and hypolophid on m2 and m3 has not occurred (Figure 10.5). The mesial surface of metaconid is unworn on m3.

Specimen NSMLL-26 (Figure 11.3-4, Table 3) is a fragment of mandible, right mandibular body of an adult individual. The rostral part is broken off at the level of the symphysis notch, between the p2 and p3 alveoli. The caudal side is broken off between the p4 and m1 alveoli. The alveolus of p4



**FIGURE 11.** *Stephanorhinus kirchbergensis*; Chumysh River at Kytmanovo (Kytmanovo District, Altay Territory, southeast Western Siberia); the vertical right ramus of a mandible NSMLL-26. 1, posterior view. 2, lingual view. The horizontal right body of a mandible NSMLL-27. 3, buccal view. 4, occlusal view. Scale bar ruled in centimeters.

bears the remains of roots. The p3 (STL6) is preserved in the jaw. Valleys are V-shaped. A weakly developed cingulid is present on the buccal and lingual sides of hypolophid. The estimated biological age of the individual is 6–9 years.

Specimen NSMLL-27 (Figure 11.1-2, Table 3) is a fragment of mandible, right vertical ramus of an adult individual. The vertical ramus is relatively broad with a strongly developed area of attachment of the masseteric muscles to the masseteric fossa. The coronoid process is directed upwards. Its tip bends in the aboral direction, as it is frequently observed in *Coelodonta antiquitatis*. The condyle is very wide (transverse diameter is 112 mm) with a visible lateral asymmetry. The medial edge of the condyle is sharp, with a rectangular outline. In *C. antiquitatis*, this edge becomes rounded towards the vertical axis of the vertical ramus when approaching the condyle and it takes a convex shape.

#### Isolated Teeth

Upper teeth are large, brachyodont, with smooth enamel, and without a clear pattern of

**TABLE 5.** Comparison of the upper permanent teeth of *Stephanorhinus kirchbergensis* and *Coelodonta antiquitatis* of the Middle and Upper Pleistocene from the Altay Territory and Novosibirsk, and Tomsk Provinces of southeastern Western Siberia versus European and Chinese areas. All measurements are in mm. Sample sizes are given in parentheses. Available in zipped download at <https://palaeo-electronica.org/content/2021/3322-stephanorhinus-kirchbergensis-in-siberia>.

enamel prisms. Medial valleys are open, except in two M3 (NSMLL-4 and IAE BB-1), for which they are closed. The occlusal surface of the teeth is concave, except for the specimen PM TSU 1/396 that displays a flat occlusal surface.

The upper left M1 PM TSU 1/396 (Figure 10.1-2, Table 5) is well preserved, with some enamel breakages on the parastyle and metastyle. The roots are preserved. The tooth is similar to PM TSU 5/3495 from Krasniy Yar (Shpansky and Billia, 2012) in the degree of wear and morphology. The protoloph and hypocone are bulbous. The front wall of the protoloph bears part of a cingulum. The enamel is smooth, with a porcelain gloss. The antecrochet is absent, the crista is poorly developed, and the crochet is well developed and quadrate-shaped.

Specimen NSMLL-5 (Figure 12.1, Table 5) is an upper left M2 that has an average stage of wear (STU6). Crochet is well developed, without virgations. Crista and antecrochet are absent. The cingulum is clear, present on the mesial part of the tooth, and only slightly developed on the lingual side. The protocone is clearly separated. The style of the paracone is well developed from the side of ectoloph. The buccal side of the tooth is significantly higher than the lingual side. The ectoloph is

inclined in the lingual direction and serrated. The relief of the ectoloph is high. Apices of the paracone and metacone are rounded. Fragments of a thin layer of cementum are present.

Specimen NSMLL-1 (Figure 12.2, Table 5) is an upper right M2 that is moderately worn (STU5). The crochet is well developed, without virgations. The crista is well developed, with double virgation. Antecrochet is absent. The cingulum is present on the mesial part of the tooth, while it is slightly visible on the lingual part of the tooth. The protocone is not isolated. The style of the paracone is well developed from the side of the ectoloph. The buccal side of the tooth is significantly higher than the lingual side. The ectoloph is inclined in the lingual direction and serrated. The relief of the ectoloph is high. The apices of the paracone and metacone are rounded.

Specimen NSMLL-6 (Figure 13.1, Table 5) is an upper left P4 that is more than 50% worn (STU8). The crochet is well developed, without virgations. The crista is absent. Antecrochet is absent. A poorly-defined cingulum is observed on the lingual part of the tooth. The protocone is not isolated. The occlusal surface is concave. The relief of the ectoloph is high. Apices of the paracone and metacone are rounded.

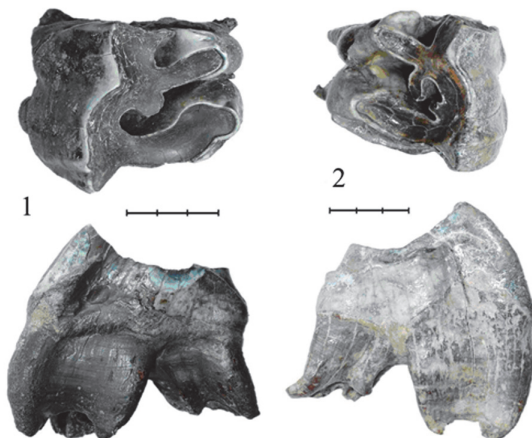


**FIGURE 12.** *Stephanorhinus kirchbergensis*; Chumysh River, at Kytmanovo (Kytmanovo District, Altay Territory, southeast Western Siberia). 1, second left upper molar M2, NSMLL-5. 2, second right upper molar M2, NSMLL-1; occlusal and anterior views. Scale bar ruled in centimeters.



**FIGURE 13.** *Stephanorhinus kirchbergensis*; Chumysh River, at Kytmanovo (Kytmanovo District, Altay Territory, southeast Western Siberia). 1, fourth left upper permanent premolar P4, NSMLL-6. 2, fourth right upper permanent premolar P4, NSMLL-2; occlusal and anterior views. Scale bar ruled in centimeters.

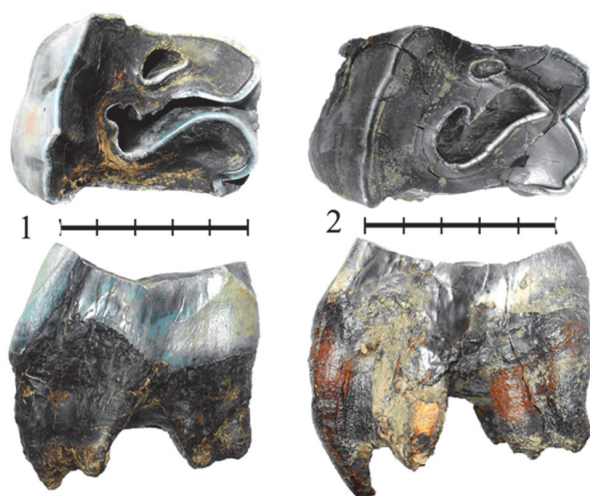


**FIGURE 14.** *Stephanorhinus kirchbergensis*; Chumysh River, at Kytmanovo (Kytmanovo District, Altay Territory, southeast Western Siberia). 1, fourth left upper permanent premolar P4, NSMML-7. 2, fourth left upper permanent premolar P4, NSMML-8; occlusal and anterior views. Scale bar ruled in centimeters.

Specimen NSMML-2 (Figure 13.2, Table 5) is an upper right P4 that is more than 50% worn (STU8), with partially destroyed protocone and parastyle. Crochet is well developed, without virgations. Crista and antecrochet are absent. A poorly-defined cingulum is observed on the lingual part of the tooth. The protocone is not isolated. The occlusal surface is concave. The relief of the ectoloph is high. The apex of the metacone is sharp. Fragments of a thin layer of cementum are present.

Specimen NSMML-7 (Figure 14.1, Table 5) is an upper left P4 that is 50% worn (STU7). Crochet is well developed, with double virgation. The crista is well developed, without virgations. Antecrochet is absent. Well-developed cingula are present on the mesial and lingual sides of the tooth. The protocone is not isolated. The relief of the ectoloph is high. The apices of the paracone and metacone are sharp.

Specimen NSMML-8 (Figure 14.2, Table 5) is an upper left P4 worn more than 50% (STU8). The crochet is well developed, and unlike the crista, without virgations. Antecrochet is absent. Well-developed cingula are observed on the mesial and lingual sides of the tooth. The protocone is not isolated. The relief of the ectoloph is high. The apices of the paracone and metacone are rounded.

Specimen NSMML-3 (Figure 15.2, Table 5) is an upper left M3 that is moderately worn (STU6), with destroyed protocone and parastyle. The crochet is well developed, without virgations. The sin-

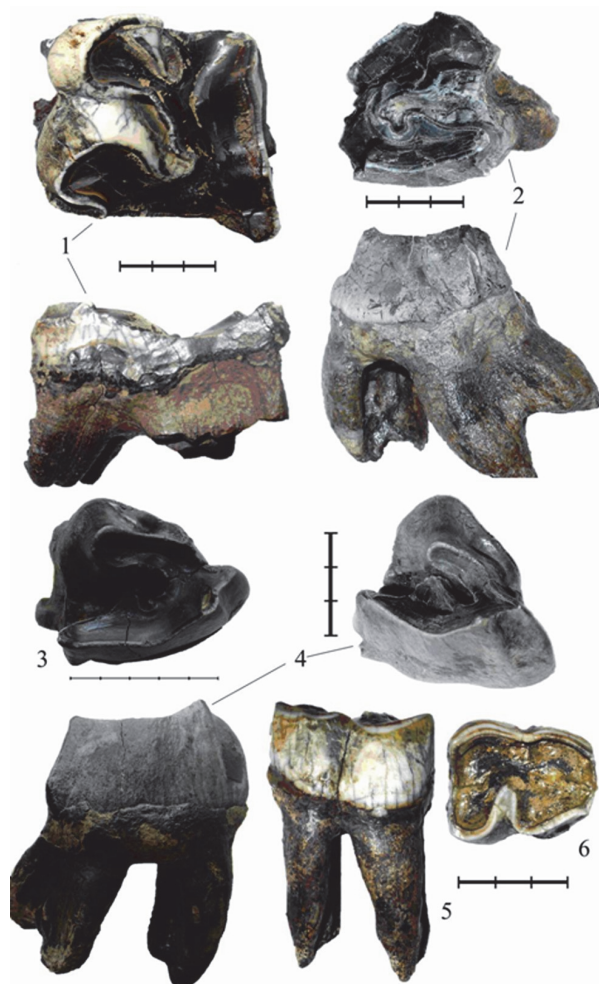


**FIGURE 15.** *Stephanorhinus kirchbergensis*; 1, Ob River (Novosibirsk Province, southeast Western Siberia); second right upper molar M2, NSMML 21052, occlusal and anterior views. 2, Chumysh River, at Kytmanovo (Kytmanovo District, Altay Territory, southeast Western Siberia); third right upper molar M3, NSMML-3, occlusal and buccal views. 3, third left upper molar M3, NSMML-4, occlusal view. 4, third left upper molar M3, IAE BB-1, Berdsk (Novosibirsk Province, southeast Western Siberia), occlusal and buccal views. 5 and 6, Omsk (Omsk Province, southeast Western Siberia), third left lower premolar p4, Sk\_oms1. 5, buccal view. 6, occlusal view. Scale bar ruled in centimeters.

gle crista is poorly developed, without virgations. Antecrochet is absent. The tooth is triangular with merged ecto- and metaloph in the dorsal section. The relief of the occlusal surface is high. The apices of the paracone and metacone are destroyed.

Specimen NSMML 21052 (Figure 15.1, Table 5) is an upper right M2 that is more than 50% worn (STU8). The ectoloph is preserved as a narrow stripe because of the high degree of wear but it is

serrated. The relief of the ectoloph is high. The apices of the paracone and metacone are sharp. The cingulum is poorly developed on the lingual side. The protocone is not isolated.

Specimen NSMLL-4 (Figure 15.4, Table 5) is an upper left M3 that is moderately worn (STU5). The roots of the tooth are broken. The crochet and crista are well developed, without virgations. Antecrochet is absent. The median valley is closed. The cingulum is present only on the mesial side. The protocone is not isolated. The style of the paracone is well developed from the side of the ectoloph. The relief of the ectoloph is high. The apices of the paracone and metacone are rounded. Fragments of a thin layer of cementum are present. The tooth is triangular with merged ecto- and metaloph in the dorsal section.

Specimen IAE BB-1 (Figure 15.3, Table 5) is an upper left molar M3 that is moderately worn (STU6). The crochet and crista are well developed, without virgations. Antecrochet is absent. The median valley is closed. A well-defined cingulum is present on the mesial side of the tooth. The protocone is not isolated. The style of the paracone is well developed from the side of ectoloph. The relief of the ectoloph is high. The apices of the paracone and metacone are rounded. Fragments of a thin layer of cementum are present. The tooth is triangular with merged ecto- and metaloph in the dorsal section.

Specimen Sk\_oms1. (Figure 15.5-6, Table 3) is a lower left p4. The tooth is large and heavily worn to the level of the distal valley. The crown is vertically convex and barrel-shaped. The valley between lophids is well defined. The lophids are convex on the occlusal surface. There is a facet on the buccal side, which forms an acute angle to the occlusal surface. This facet appears in rhinoceroses that are characterized by a brachyodont dentition.

The lower left p3 PM TSU 1/395 (Table 3) is a tooth that is heavily worn below the level of valleys. The enamel is preserved only on the buccal wall of the hypolophid. The enamel is light gray, smooth, and porcelaneous, without wrinkles or cementum. The front edge of the metalophid has a horizontal cylinder-shaped bulbosity at the base. The metalophid is narrower than the hypolophid.

### Postcranial material

Specimen NSMLL-109 (Figure 16.1-3, Table 6) is a well-preserved left ulna that lacks the distal epiphysis. The bone is long and gracile. Its absolute size is smaller than the equivalent bone from

the Taubach (Kahlke, 1977). In *Coelodonta antiquitatis*, the mediolateral diameter of some individuals is considerably larger than that. In the given specimen, the proc. coracoideus slightly rises upwards (Figure 16.1), which is a characteristic of *S. kirchbergensis*. In *C. antiquitatis* the proc. coracoideus points downwards and the proximal part of the olecranon has a wide flat area, which abruptly expands towards the olecranon tubercle on the medial side. This expansion forms a sharp edge, pointed medially. In NSMLL-109, the proximal part of the olecranon is relatively narrow with a sharp-edged ridge along the dorsal surface, and a smooth extension on the medial side towards the olecranon tubercle not forming the medial ridge (Figure 16.2). In *C. antiquitatis*, a notch extends from outside of the ventro-medial projection of incisura semilunaris, and around its distal portion, which sharply separates it from the rest of the joint surface of the diaphysis. In NSMLL-109, this notch is not observed. The transition between the joint and the diaphysis is smooth (Figure 16.3). There is a ridge along the lateral side of the diaphysis from the incisura semilunaris to the distal epiphysis with a gap in the middle. In the area of the gap, the diaphysis is relatively sharp and forms a dihedral angle with a rounded tip (Figure 16.2). In *C. antiquitatis*, that area of the diaphysis is flat. In NSMLL-109, the palmar wall of the diaphysis is straight and, unlike *C. antiquitatis*, without flexure.

Specimen IAE CHU-108 (Figure 17.1-4, Table 7) is a well-preserved right radius of *Stephanorhinus kirchbergensis*. It has a large absolute length of 436 mm; it is larger than similar bones of *Coelodonta antiquitatis* (maximum length for the specimen from Krasniy Yar, Tomsk Province, is 424 mm) (Shpansky, 2014). Specimen IAE CHU-108 appears more slender, the transverse diameter of the proximal epiphysis index being 25.2% of the total length of the bone, while the average values are 26.2% and 29.7% for *S. kirchbergensis* and *C. antiquitatis*, respectively (Guérin, 1980). Absolute values for the measurements and indices of the relative proportions correspond to the values typical for *S. kirchbergensis*. In *C. antiquitatis*, the transition from the ventral edge of the lateral part of the proximal epiphysis facet to the lateral edge is smooth, rounded, and convex and the intersection of the lateral and dorsal edges forms an obtuse angle of around 120°. In IAE CHU-108, the ventral edge of the proximal facet of the lateral part is straight and considerably shifted towards the medial facet, which makes the ventral edge appear shorter. The transition in the lateral edge occurs by



**FIGURE 16.** *Stephanorhinus kirchbergensis*; Chumysh River at Kytmanovo (Kytmanovo District, Altay Territory, southeast Western Siberia). The left ulna, NSMLL-109. 1, medial view. 2, anterior view. 3, lateral view. The right astragalus, NSMLL-107. 4, dorsal view. 5, plantar view. Scale bar ruled in centimeters.

**TABLE 6.** Measurements of the ulna of *Stephanorhinus kirchbergensis* and *Coelodonta antiquitatis* from southeastern Western Siberia and Europe. All measurements are in mm. Sample sizes are given in parentheses. The following measurements were used: maximum length in the sagittal plane (ML); antero-posterior diameter of the proximal epiphysis (APD); antero-posterior diameter of the distal epiphysis (APDde); transverse diameter of the distal epiphysis (TDde); transverse diameter of the diaphysis in the middle (mTDd); antero-posterior diameter of the diaphysis in the middle (mAPDd); transverse diameter of the olecranon (TD olecr.); antero-posterior diameter of the olecranon (APD olecr.); transverse diameter of the proximal joint (TD artic. prox.); maximum height of the proximal joint (H artic. prox.).

Dimensions	<i>S. kirchbergensis</i>			<i>C. antiquitatis</i>		
	Altay Territory, NSMLL-109	Europe, Taubach (Kahlke, 1977)	Europe (Guérin, 1980 tab. 131)		Europe (Guérin, 1980 tab. 131)	
			Range	Mean	Range	Mean
ML					456 - 543	494.5(21)
TD olecr.	72		67 - 68	67.5(2)	57 - 102	84.2(13)
APD olecr.	90		103 - 107	104.5(3)	90 - 120	106.4(23)
TD artic.prox.	98	101.8	91 - 94	92.5(2)	75 - 109	92.5(30)
APD	175		140 - 157	148.5(2)	121 - 195	159.1(26)
mTDd	43	49.9	51 - 52	51.5(2)	44 - 68	55.4(18)
mAPDd	41	46.3	52	52(2)	41.5 - 60	51.8(18)
TDde				40	41 - 67	53.8(16)
APDde				77	60 - 92	76.2(15)
H artic. prox.	113	106.5				



**FIGURE 17.** *Stephanorhinus kirchbergensis*; Chumysh River at Kytmanovo (Kytmanovo District, Altay Territory, southeast Western Siberia). The right radius, IAE CHU-108. 1, anterior view. 2, lateral view. 3, proximal view. 4, distal view. The left tibia, NSMLL-110. 5, distal view. 6, proximal view. 7, anterior view. 8, posterior view. Scale bar ruled in centimeters.

a rounded obtuse angle, around  $130^\circ$ . The lateral edge is straight and intersects a dorsal edge at an acute rounded angle, less than  $90^\circ$  (Figure 17.3). This morphology of the radius proximal joint is typical of *S. kirchbergensis* (Guérin, 1980). In *C. antiquitatis*, the tuberosity on the dorsal surface of the distal epiphysis is divided by a broad, shallow sagittal groove. In IAE CHU-108, the tuberosity on the dorsal surface of the distal epiphysis is flat, without a visible separation (Figure 17.1), which is characteristic of *S. kirchbergensis* (Guérin, 1980). In *C. antiquitatis*, the dorsal ridge separating the facets for lunate and scaphoid bones on the surface of the distal joint is well defined, especially on the anterior part of the joint surface (Gromova, 1950). In IAE CHU-108, the dorsal ridge is almost invisible (Figure 17.4).

Specimens NSMLL-102 and GR PC 203 are well-preserved left Mc II and GR PC 214 is a right Mc II that is damaged in the area of the distal joint and near the facet for Mc III (Figures 18.1-4, 19.1-8, Table 8). All of the bones listed above are large (Table 8) and considerably exceed the dimensions of the *Coelodonta antiquitatis* bones. Moreover, the bones of *Stephanorhinus kirchbergensis* are more slender. Their three main transverse diameter indices are considerably smaller than those in *C. antiquitatis*. The surface of the Mc II proximal joint from the lateral side has a sharp angle between trapezoid and magnum facets. In *C. antiquitatis*, it forms an angle of around  $100^\circ$ , while in NSMLL-102 and GR PC 203, it is less than  $90^\circ$  (Figures 18.3, 19.3). The lateral facet for Mc III in *C. antiquitatis* has a more abrupt expansion than in *S. kirchbergensis* (Guérin, 1980) (Figures 18.2, 19.2). The cross-section of the diaphysis is more elliptic with a small keel along the volar surface, especially in GR PC 214 (Figure 19.7). The diaphysis is thicker from the medial side, which characterizes *S. kirchbergensis* (Guérin, 1980). In *C. antiquitatis*, the cross-section of the diaphysis has a broadly elliptic shape with a relatively sharp edge on the medial side and the surface of the diaphysis on the volar side is either flat or tuberos (Guérin, 1980).

Specimens IAE TRD-17 and IAE TRD-18 (Figures 18.5-8, 20.1-4, Table 9) are left Mc IV. Specimen IAE TRD-18 has lengthwise damage in the area of the distal epiphysis, while specimen IAE TRD-17 is well preserved. The bones have a large relative length and are considerably larger than those in *Coelodonta antiquitatis*. At the same time, the bones are more slender; their epiphysis and diaphysis indices are much smaller than those in *C. antiquitatis* (Table 9). In *C. antiquitatis*, the volar side of the proximal joint (the closest distance between the facet for Mc V and volar facet for Mc III) is always smaller than the dorsal side of the joint (the closest distance between the facet for Mc V and dorsal facet for Mc III). Both dorsal and volar sides of the joint in these specimens have approximately the same length, just as in *Stephanorhinus kirchbergensis* (Guérin, 1980). In *C. antiquitatis*, the sides of the two facets for articulation with Mc III are usually fused in the medial part of the proximal epiphysis, forming a dihedral angle, but may be separated by a small groove. In *S. kirchbergensis*, the groove is present between the facets. In *C. antiquitatis*, the palmar facet for Mc III is usually round while the dorsal palmar facet is relatively wider (the height is more than half the width). In IAE TRD-17 and IAE TRD-18, the palmar facet is

**TABLE 7.** Measurements of the radius of *Stephanorhinus kirchbergensis* and *Coelodonta antiquitatis* from southeastern Western Siberia and Europe. All measurements are in mm. Sample sizes are given in parentheses. The following measurements were used: maximum length in the sagittal plane (ML); antero-posterior diameter of the proximal epiphysis (APD); transverse diameter of the proximal epiphysis (TD); antero-posterior diameter of the distal epiphysis (APDde); transverse diameter of the distal epiphysis (TDde); transverse diameter of the diaphysis in the middle (mTDd).

Dimensions	<i>S. kirchbergensis</i>				<i>C. antiquitatis</i>			
	Altay Territory, IAE CHU-108	Europe (Guérin, 1980 tab. 130)		Europe (Guérin, 1980 tab. 130)	Altay Territory and Novosibirsk Province, IAE: Krasniy Yar, Taradanovo, Chumysh			
		Range	Mean	Range	Mean	Range	Mean	
ML	436	408 - 445	421.8(5)	334 - 413	380.4(81)	335 - 405	379.1(13)	
APD	88	68 - 87	74.9(18)	55 - 93	77.5(106)	68.5 - 91.5	81.6(13)	
TD	110	102 - 119	110.4(18)	97 - 126	112.8(109)	95 - 123.5	114.7(13)	
APDde	66	61 - 82	67.9(10)	62 - 92	76.6(80)	61 - 84.5	76.1(13)	
TDde	109	90.5 - 113.5	105(10)	95 - 142	117.7(84)	94 - 130.5	118.6(13)	
mTDd	57	53 - 65	58.7(9)	54 - 75.5	63.4(103)	52.7 - 73	63.7(13)	
Indexes, %								
TD/ML	25.2		26.2(5)		29.7(81)	28.4 - 32.3	30.3(13)	
mTDd/ML	13.1		13.9(5)		16.7(81)	15.4 - 18	16.8(13)	
TDde/ML	25		24.9(5)		30.9(81)	28.1 - 32.5	31.3(13)	

high and relatively narrow, while the dorsal one is low and long (the width is about a third of the height), with a small inclination towards the proximal edge (Figures 18.7, 20.3), as mentioned for *S. kirchbergensis* (Guérin, 1980). In IAE TRD-17 and IAE TRD-18, the tuberosity for attachment of the interosseous muscle on the medial surface is relatively weak (Figures 18.5, 20.1), which is not typical of *C. antiquitatis* (Belyaeva, 1966). In *C. antiquitatis*, the cross-section of the diaphysis is relatively thick and triangular, with rounded angles. In *S. kirchbergensis*, just as in IAE TRD-17 and IAE TRD-18, the cross-section of the Mc IV diaphysis is trapezoidal in shape with a large base on the dorsal side and a very acute angle at the base of the lateral side (Guérin, 1980).

Specimen PM TSU 5/5197 is a Mc III with a strongly flattened diaphysis in the dorsoventral direction. The distal end of the bone is absent (Figure 21.3-4). The bone is large (Table 10), significantly exceeding the previously described specimen PM TSU 5/2723 (Figure 21.1-2) (Shpan-sky and Billia, 2012), but smaller than a massive bone from Rybinsk (Belyaeva, 1940).

Specimen NSMLL-110 (Figure 17.5-8, Table 11) consists of a left tibia and a left fibula. The bones are fused and well preserved. The fibula has the following sizes: absolute length is 351 mm (in *Coelodonta tologiensis*, 340 mm [Belyaeva,

1966]); its mediolateral width of the proximal epiphysis is 28 mm; its transverse width of the proximal epiphysis is 44 mm; its mediolateral width of the diaphysis is 32 mm; its transverse diameter of the distal end is 54 mm; and its transverse width index is 15.4% (in *Coelodonta antiquitatis*, it is less than 16% [Gromova, 1950]). Tibia length of NSMLL-110 is 444 mm, which exceeds the size of *C. antiquitatis* (maximal length for the Krasniy Yar locality of Tomsk Province, West Siberia, is 438 mm) (Shpan-sky, 2014). The tibia of *S. kirchbergensis* appears more slender than that of *C. antiquitatis* (Table 11; indices of proximal and distal epiphyses). Absolute values for measurements of tibia NSMLL-110 and indices of relative proportions correspond to the values typical of *S. kirchbergensis*. Tuberositas on the proximal epiphysis of tibia is relatively short and less massive (maximum mediolateral width of tuberositas to width of the proximal epiphysis is 36%). Therefore, the width of the proximal epiphysis is significantly larger than the transverse diameter (Figure 17.6), which is a characteristic of *Stephanorhinus kirchbergensis*. In *C. antiquitatis*, maximum width of tuberositas is about 50% of the width of the proximal epiphysis, which makes the width of the proximal epiphysis less than its transverse diameter. In *S. kirchbergensis*, and in NSMLL-110, the medial edge of the tibia distal

epiphysis is convex (Figure 17.5), while in *C. antiquitatis*, it is concave (Gromova, 1950).

Specimen NSMLL-107 (Figure 16.4-5, Table 12) is a right astragalus. The bone is large, close to the size of the specimen from Krasniy Yar (Tomsk Province) and Western Europe (Table 11). The ratio of the height of the bone to its width is 93.3%; the transverse diameter compared to the width is 58.5%. The average values for *Stephanorhinus kirchbergensis* are 94.2% and 65.9%, respectively; for *Coelodonta antiquitatis*, they are 90.8% and 65.2%, respectively (Guérin, 1980). The absolute values for the measurements and proportional indices for *S. kirchbergensis* usually exceed the values for *C. antiquitatis*, but some large individuals of woolly rhinoceros may display similar sizes. In *S. kirchbergensis*, just as in NSMLL-110, the dorsal part of the lateral calcaneal facet has a sharp posterior edge without transition into the ventral part (Figure 16.5), as in *C. antiquitatis* (Shpansky and Billia, 2012).

Specimens PM TSU 5/2538 and PM TSU 5/3063 are right naviculars of adult individuals (Figure 22). Because the bones of the postcranial skeleton of *Stephanorhinus kirchbergensis* can often be found together with the remains of a woolly rhinoceros in alluvial localities during redeposition, we compared the characteristics and features of the navicular bone of these species (Table 13).

Specimen NSMLL-101 (Figure 23.1-4, Table 14) is a left Mt II. The specimen is slightly worn in the area of the proximal epiphysis and has a large absolute length. The bone appears slender; its proportions are close to the average of *Stephanorhinus kirchbergensis* from Europe (Guérin, 1980). Two facets conjoined with facets of Mt III are present on the lateral side of the proximal epiphysis. The dorsal facet is smaller than the plantar one, its contour is near trapezoid in shape, and the proximal edge does not exceed the proximal edge of the plantar facet. The plantar facet is trapezoid-shaped; its height is larger than its width. Both facets have an unclear outline, which is typical for *S. kirchbergensis* (Guérin, 1980). In *Coelodonta antiquitatis*, the two facets for Mt III are usually placed on the lateral side of the proximal epiphysis, but often they may be merged. If the facets are separate, the dorsal one may be either round or elliptical and proximo-distally extended. The plantar facet is usually round. The dorsal facet is placed higher than the plantar one. There is a facet for the first cuneiform on the plantar side of the proximal epiphysis. In *S. kirchbergensis*, the facet is relatively large, usually rectangular or the shape

of a flipped L (Guérin, 1980). In *C. antiquitatis*, this facet is placed high, elliptical or trapezoid, and often limited by the deep vertical groove. In NSMLL-101, the plantar facet is unclear because of the damage on this spot; the vertical groove is absent. The diaphysis of *S. kirchbergensis* is pentagonal in the dorsal plane, while four front angles may have an unclear outline, but on the plantar side there is always a clear V-shaped angle, due to the high keel along the middle part of plantar wall surface. This keel is clearly observed on NSMLL-110 (Figure 23.3), but the distal expansion of the diaphysis is relatively weaker than in other species of rhinoceroses (Guérin, 1980). In *C. antiquitatis*, the diaphysis is elliptical in the dorsal plane and more circular and its distal expansion is larger, compared to the other species of rhinoceroses (Guérin, 1980).

Specimens NSMLL-105 and IAE TRD-2 (Figures 20.5-8, 23.5-8, Table 15) are well-preserved left Mt IV. The length of those specimens is higher than in *Coelodonta antiquitatis* and Mt IV of the European samples of *Stephanorhinus kirchbergensis* (Guérin, 1980). The relative medio-lateral width of the *S. kirchbergensis* diaphysis and the epiphyses of Mt IV is less than those of *C. antiquitatis* (Table 15). In *S. kirchbergensis*, part of the dorsal edge of proximal is concave from the dorsal facet for Mt III in the lateral direction as the dorsal facet for Mt III stretches dramatically in the medio-plantar direction; we get a distinct change in the outline of the dorsal edge of the proximal facet, which has an angle of about 100°. This characteristic angle is well defined on the proximal facets of NSMLL-105 and IAE TRD-2 (Figures 20.8, 23.8). In *C. antiquitatis*, this area of the proximal facet dorsal edge is convex without sharp bends. At the same time, the outline of the proximal facet plantar edge is highly concave in NSMLL-105 and IAE TRD-2 (Figures 20.8, 23.8), which is typical of *S. kirchbergensis* and not typical for *C. antiquitatis* (Belyaeva, 1966). A calloused protuberance is well developed on the plantar side of the proximal epiphysis in NSMLL-105 and IAE TRD-2. In NSMLL-105, it rises in the proximal direction to the level of the joint surface (Figure 23.8). This is not observed on the proximal epiphysis of *C. antiquitatis*. In NSMLL-105 and IAE TRD-2, the dorsal facet is semi-elliptical and touches the edge of the proximal facet. Its width is less than half of the length. The plantar facet has the shape of an ellipse that is slightly elongated vertically; it is placed below the dorsal facet and separated from the proximal facet by a notch (Figures 20.6, 23.6), similar to *S. kirchbergensis*



**FIGURE 18.** *Stephanorhinus kirchbergensis*; Chumysh River at Kytmanovo (Kytmanovo District, Altay Territory, south-east Western Siberia). The left Mc II, NSMLL-102. 1, dorsal view. 2, lateral view. 3, volar view. 4, proximal view. Ob River at Taradanovo Village (Suzun District, Novosibirsk Province, southeast Western Siberia). The left Mc IV, IAE TRD-17. 5, dorsal view. 6, medial view. 7, volar view. 8, proximal view. Scale bar ruled in centimeters.

(Guérin, 1980). In *C. antiquitatis*, if both facets are present, the dorsal one is semicircular, with its width little larger than its height, and the plantar facet is circular. When the facets are united, the common facet is L-shaped (Guérin, 1980). In *S. kirchbergensis*, just as in NSMLL-105 and IAE TRD-2, the cross-section of the diaphysis is oval and stretched in the dorso-plantar direction without sharp inflections in the contour. In *C. antiquitatis*, the diaphysis has a round cross-section with sharp bends due to the frequent presence of sharp longitudinal ridges on the surface of the diaphysis (Guérin, 1980).

#### ODONTOLOGICAL ANALYSIS

Adaptation of some animal groups to a food base that included a high proportion of abrasive food (grass) led to significant physiological and morphological differences from those who preferred a diet with a small percentage of rough food (Clauss et al., 2008). Recent and Pleistocene rhi-

noceroses are one of the most prominent representatives that demonstrate a high degree of specialization of adaptation to different ecological environments. Therefore, considering the morphological features of the fossil material represented by *Stephanorhinus kirchbergensis*, we focused on the morphological characteristics that reflected food preferences. For greater clarity, the study was carried out by comparing *S. kirchbergensis* with the morphology of *Coelodonta antiquitatis* that lived in West Siberia. We used the methods presented in Fortelius (1982) and Clauss et al. (2008) to study the morphological differences of typical browsers and grazers based on the recent African rhinoceroses *Diceros bicornis* and *Ceratotherium simum*.

First of all, let us consider the adaptations associated with increased resistance of the teeth to abrasion caused by different dietary requirements. The considerable amount of silica in the grass and its cover of dust in the Pleistocene landscapes under arid climate significantly affected the rate of dental wear. Therefore, the appearance of hypsod-



**FIGURE 19.** *Stephanorhinus kirchbergensis*; Bijsk (Altay Territory, southeast Western Siberia). The left Mc II, GR PC-203. 1, dorsal view. 2, lateral view. 3, volar view. 4, proximal view. The right Mc II, GR PC-214, 5, dorsal view. 6, lateral view. 7, volar view. 8, proximal view. Scale bar ruled in centimeters.

**TABLE 8.** Measurements of McII of *Stephanorhinus kirchbergensis* and *Coelodonta antiquitatis* from southeastern Western Siberia and Europe. All measurements are in mm. Sample sizes are given in parentheses. The following measurements were used: maximum length in the sagittal plane (ML); antero-posterior diameter of the proximal epiphysis (APD); transverse diameter of the proximal epiphysis (TD); antero-posterior diameter of the distal epiphysis (APDde); transverse diameter of the distal epiphysis (TDde); transverse diameter of the diaphysis in the middle (mTDd).

Dimensions	<i>S. kirchbergensis</i>				<i>C. antiquitatis</i>				
	Altay Territory NSMLL-102	Altay Territory GR PC-203	Altay Territory GR PC-214	Europe (Guérin, 1980 tab. 139)	Europe (Guérin, 1980 tab. 139)	Altay Territory and Novosibirsk Province, IAE: Krasniy Yar, Taradanovo, Chumysh	Altay Territory and Novosibirsk Province, IAE: Krasniy Yar, Taradanovo, Chumysh		
				Range	Mean	Range	Mean	Range	Mean
ML	187.5	186	c194	179 – 212	195.4(13)	148 - 180	164.2(60)	144.7 - 180.4	164.3(26)
APD	46	62.5	59	42.5 – 60	48.2(12)	40 - 58	47(57)	35 – 52	44.7(26)
TD	48	58.5	61	41 – 57	48.0(12)	41 - 66.5	52.9(61)	47 – 63	54.8(26)
APDde	44	51.5		37.5 - 53.7	45.0(12)	35 - 52.5	43.1(58)	35 – 49	42.8(26)
TDde	52	52	57	45 – 56	48.9(12)	37.5 - 57	48.8(55)	41.4 - 56.5	47.7(26)
mTDd	40	40	44	33.5 - 41.5	38.6(13)	31.5 - 50	42.4(60)	37 - 48.7	42(26)
Indexes, %									
TD/ML	25.6	31.5	31.4		24.6(12)		32.2(60)	29.6 - 36.2	33.4(26)
mTDd/ML	21.3	21.5	22.7		19.7(13)		25.8(60)	23.8 - 28.7	25.5(26)
TDde/ML	27.7	28	29.4		25(12)		29.7(55)	26.2 – 32	29(26)



**FIGURE 20.** *Stephanorhinus kirchbergensis*; Ob River at Taradanovo village (Suzun District, Novosibirsk Province, southeast Western Siberia). The left Mc IV, IAE TRD-18. 1, dorsal view. 2, medial view. 3, volar view. 4, proximal view. The left Mt IV, IAE TRD-2. 5, dorsal view. 6, medial view. 7, plantar view. 8, proximal view. Scale bar ruled in centimeters.

**TABLE 9.** Measurements of McIV of *Stephanorhinus kirchbergensis* and *Coelodonta antiquitatis* from southeastern Western Siberia and Europe. All measurements are in mm. Sample sizes are given in parentheses. The following measurements were used: maximum length in the sagittal plane (ML); antero-posterior diameter of the proximal epiphysis (APD); transverse diameter of the proximal epiphysis (TD); antero-posterior diameter of the distal epiphysis (APDde); transverse diameter of the distal epiphysis (TDde); transverse diameter of the diaphysis in the middle (mTDd).

Dimensions	<i>S. kirchbergensis</i>				<i>C. antiquitatis</i>			
	Novosibirsk Province, IAE TRD-17	Novosibirsk Province, IAE TRD-18	Europe (Guérin, 1980 tab. 141)		Europe (Guérin, 1980 tab. 141)		Altay Territory and Novosibirsk Province, IAE: Krasniy Yar, Taradanovo, Chumysh	
			Range	Mean	Range	Mean	Range	Mean
ML	199	188.5	172.5 - 193	182.1(9)	126.5 - 176.5	151.1(59)	136 - 163.5	151.3(25)
APD	52	51.5	39 - 51	43.3(12)	39 - 52	45(52)	35 - 49	44.9(25)
TD	55.5	51	48 - 62	51.6(12)	41 - 62.5	53.3(57)	47 - 61	55.4(25)
APDde	51	0	41 - 50	44.9(9)	34 - 48	42.3(50)	37 - 45	41.5(25)
TDde	56	52.5	43 - 51	47.3(8)	42 - 62.5	47.9(58)	43 - 55	49.6(25)
mTDd	44.5	40	34 - 42	38.1(10)	32 - 46	37.6(59)	30.5 - 48	38.6(25)
Indexes, %								
TD/ML	27.9	27		28.3(9)		35.3(57)	34.6 - 38.4	36.6(25)
mTDd/ML	22.4	21.2		20.9(9)		24.9(59)	22.4 - 29.4	25.5(25)
TDde/ML	28.1	27.9		26(8)		31.7(58)	31.2 - 35.6	32.8(25)



**FIGURE 21.** *Stephanorhinus kirchbergensis*; Tobol Horizon level (Middle Pleistocene), Ob River at Krasniy Yar (Tomsk Province, southeast Western Siberia). The right Mc III, PM TSU 5/5197. 1, lateral view. 2, dorsal view. The left Mc III, PM TSU 5/2723. 3, lateral view. 4, dorsal view. Scale bar ruled in centimeters.

only, as a result of adaptation to increased wear of the teeth, is observed in many groups of animals. We use the description of the morphological differences between hypsodont and brachyodont types of teeth in rhinos (Fortelius, 1982). The upper teeth described here show the main features of the brachyodont type, different from the characteristics

of the hypsodont type observed in *Coelodonta antiquitatis*.

The occlusal surface of the upper teeth of *S. kirchbergensis* is concave (Figure 24.3); in *Coelodonta antiquitatis*, the occlusal surface is flat (Figure 24.4). Up to STU7, the buccal side of the upper teeth of *S. kirchbergensis* is higher than the lingual and highly inclined to the lingual side, i.e., there is a bucco-lingual constriction in the occlusal area of the crown in slightly worn teeth (Figure 12.1-2; mesial view). Teeth of this type are characterized by uneven wear of the occlusal surface. After STU7, the crown height on the buccal and lingual sides becomes equal (Figure 14.1), and the buccal side becomes shorter than the lingual in the following stages (Figures 13.1-2, 14.2, 15.1). In *C. antiquitatis*, almost vertical buccal and lingual walls have nearly equal height, and wear is equal. In *S. kirchbergensis*, the ectoloph of all upper teeth is serrated. In *C. antiquitatis*, the ectoloph is straight. In *S. kirchbergensis*, secondary folds of all upper premolars and molars do not merge with each other until the very last stages of wear and do not form closed inner valleys. In *C. antiquitatis*, the secondary folds usually merge in the very first stages of wear, forming the closed inner valleys. In some specimens of *S. kirchbergensis*, styles are

**TABLE 10.** Measurements of McIII of *Stephanorhinus kirchbergensis* and *Coelodonta antiquitatis* from southeastern Western Siberia and Europe. All measurements are in mm. Sample sizes are given in parentheses. The following measurements were used: maximum length in the sagittal plane (ML); antero-posterior diameter of the proximal epiphysis (APD); transverse diameter of the proximal epiphysis (TD); antero-posterior diameter of the distal epiphysis (APDde); transverse diameter of the distal epiphysis (TDde); transverse diameter of the diaphysis in the middle (mTDd); transverse diameter of the distal joint (TDdj).

Dimensions	<i>S. kirchbergensis</i>					<i>C. antiquitatis</i>			
	Tomsk Province, Krasniy Yar, PM TSU 5/5197	Krasniy Yar (Shpansky and Billia, 2012) PM TSU 5/2723	Rybinsk (Beljaeva, 1939)	Taubach (Kalke, 1977)	Western Europe: (Guérin, 1980, tab. 140) Range Mean	Tomsk Province, Krasniy Yar (QIII) PM TSU n=7	Western Europe: (Guérin, 1980, tab. 140) Range Mean		
ML	C186	229	225	204.2	206-250.5 225.2(13)	164-198	162-213	189(79)	
APD	C50	56.6	64	63.7-67.8	50-59 54.2(13)	42-58	42.5-61.5	52.2(80)	
TD	70	63	80	63.7-67.8	58-71 63.9(17)	58.2-79	59.5-79	68.2(90)	
APDde	–	56	64		48-58.5 52.8(14)	41.8-55	44-57.5	50.8(68)	
TDde	–	80.4	90	73.9	64.5-83 73.8(14)	55-71	57.5-74	65.8(77)	
TDdj	–	64	70	59.1	52-64.5 59.6(13)	–	49-65	56.1(77)	
mTDd	67.5	60.5	72	53.5-55.7	54-70.5 61.4(16)	48-58	46-66	56.4(86)	
Indexes, %									
TD/ ML	–	27.5	35.6	31.2	28.4	33-39.9		36.1(79)	
TDde/ ML	–	35.1	40	36.2	32.8	31.9-36.2		34.8(77)	
mTDd/ ML	–	26.4	31.1	26.2	27.3	28.2-30.1		29.9(79)	

**TABLE 11.** Measurements of tibia of *Stephanorhinus kirchbergensis* and *Coelodonta antiquitatis* from southeastern Western Siberia and Europe. All measurements are in mm. Sample sizes are given in parentheses. The following measurements were used: maximum length in the sagittal plane (ML); antero-posterior diameter of the proximal epiphysis (APD); transverse diameter of the proximal epiphysis (TD); antero-posterior diameter of the distal epiphysis (APDde); transverse diameter of the distal epiphysis (TDde); transverse diameter of the diaphysis in the middle (mTDd); transverse diameter of the diaphysis in the middle (mTDd); antero-posterior diameter of the diaphysis in the middle (mAPDd); transverse diameter of the tuberositas tibia (TDtt).

Dimensions	<i>S. kirchbergensis</i>			<i>C. antiquitatis</i>			
	Altay Territory, NSMML-110	Europe (Guérin, 1980 tab. 144)		Europe (Guérin, 1980 tab. 144)		Altay Territory and Novosibirsk Province IAE: Krasniy Yar, Taradanovo, Chumysh	
		Range	Mean	Range	Mean	Range	Mean
ML	444	404 - 457	429(3)	323.5 - 433	381.1(67)	364 - 424	394.5(4)
APD	133		137.5(1)	87 - 157.5	136.8(42)	125 - 156	141.3(4)
TD	149		136(1)	111 - 163	133.4(50)	119 - 147	134.4(4)
APDde	90	75.5 - 92	85.6(12)	70 - 98	82.3(88)	77 - 91.5	85.3(4)
TDde	122.5	105 - 128	111.8(12)	92 - 127	106.8(88)	101 - 120	109.4(4)
mAPDd	62	60.5 - 69.5	64.4(5)	51 - 77	63.2(82)	57 - 67	64(4)
mTDd	69	63.5 - 80	70.5(5)	59 - 82.5	70.1(85)	65 - 73	69.3(4)
TDtt	54					60 - 74	66.8(4)
Indexes, %							
TD/ML	33.6		31.7(1)		35(50)	32.3 - 36.5	34(4)
mTDd/ML	14		16.4(3)		18.4(67)	15.3 - 17.3	16.2(4)
TDde/ML	27.6		26(3)		28(67)	26.2 - 28.6	27.7(4)
APD/ML	30		32.1(1)		35.9(42)	34.1 - 37.9	35.8(4)
mAPDd/ML	15.5		15(3)		16.6(67)	17.2 - 17.9	17.6(4)
APDde/ML	20.3		20(3)		21.6(67)	20.2 - 23.6	21.6(4)
TDtt/TD	36.2					43.8 - 54.6	49.8(4)

**TABLE 12.** Measurements of the astragalus of *Stephanorhinus kirchbergensis* and *Coelodonta antiquitatis* from southeastern Western Siberia and Europe. All measurements are in mm. Sample sizes are given in parentheses. The following measurements were used: maximum transverse diameter measured perpendicularly to the vertical axis of the astragalus (ATD); maximum height, measured perpendicularly to the first diameter of the astragalus (AH); transverse diameter of distal joint of the astragalus (ATD artic. dist.); transverse diameter of distal part of the astragalus below the collar (ATD max dist.).

Dimensions	<i>S. kirchbergensis</i>				<i>C. antiquitatis</i>		
	Altay Territory, NSMML-107	Tomsk Province, Krasniy Yar (Shpansky and Billia, 2012) PM TSU 5/740	Europe (Guérin, 1980 tab. 145)		Tomsk Province, Krasniy Yar (Shpansky and Billia, 2012) n=39	Europe (Guérin, 1980 tab. 145)	
			Range	Mean		Range	Mean
ATD	112	113	93 - 113	101.7(31)	82-111	84 - 112	95.7(112)
AH	104.5	104	85 - 105	95.8(29)	79-98	77 - 102	87(112)
ATD artic. dist.	93	93	74 - 93	84.7(29)		68 - 91	80.9(107)
ATD maxi dist.	97.5	96	79 - 99	89(30)	85-98	75 - 97	85.1(108)

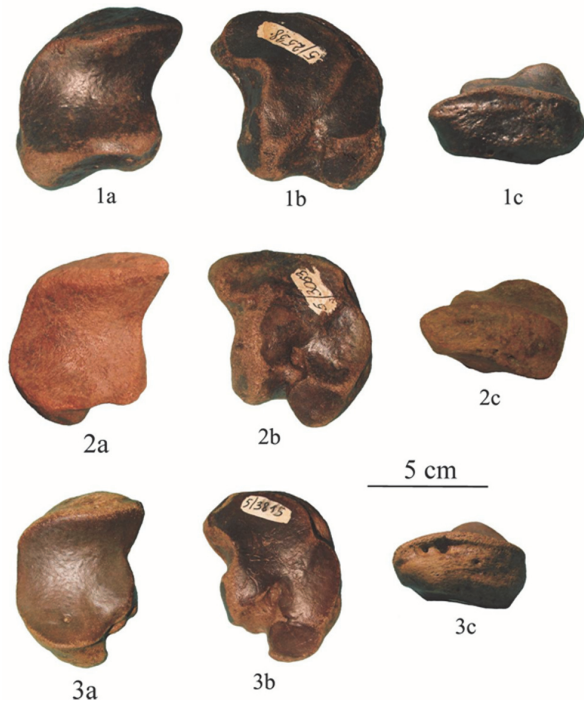


**FIGURE 22.** The navicular: *Stephanorhinus kirchbergensis*, Tobol Horizon level (Middle Pleistocene), Ob River at Krasniy Yar (Tomsk Province, southeast Western Siberia). 1, PM TSU 5/2538. 2, PM TSU 5/3063. *Coelodonta antiquitatis*, Karginian Horizon, Ob River at Krasniy Yar (Tomsk Province, southeast Western Siberia), 3, PM TSU 5/3815. a, proximal view. b, distal view. c, dorsal-medial view.

isolated. For example, isolation of the protocone is observed (Figure 12.1; occlusal view). In *C. antiquitatis*, styles are not isolated. In *S. kirchbergensis*,

the thickness of enamel is uneven along the perimeter of the tooth. It is thicker on the buccal and lingual sides. In *C. antiquitatis*, the thickness of the enamel is even along the tooth perimeter. In *S. kirchbergensis*, the shape of M3 in the dorsal plane is close to triangular, with merged ecto- and metalophs (Figure 15.2-4). In *C. antiquitatis*, the M3 cross-section is quadrate in shape, and the metaloph is often separated from the ectoloph. In all lower teeth of *S. kirchbergensis*, the lophids are convex on the occlusal side. In *C. antiquitatis*, lophids are flattened on the occlusal side. All lower teeth of *S. kirchbergensis* are convex on the buccal side, i.e., there is a smooth expansion from the occlusal part of the crown and a smooth constriction to the root. In *C. antiquitatis*, the walls on the buccal and lingual sides are almost vertical and flattened. All of the upper and lower teeth of *S. kirchbergensis* are characterized by relatively smooth enamel without a clear pattern of enamel prisms, by the absence of rugosity, and by the rare presence of cementum. In *C. antiquitatis*, the enamel surface is rough, generally with a distinct pattern of enamel prisms or wrinkling. Cementum is retained and often covers a large portion of the tooth crown in *C. antiquitatis*.

Further, it is necessary to review the results of adaptations associated with different ways of grinding the food for brachyodont and hypsodont types of teeth. The chewing process of brachyodont teeth is in two phases (Fortelius, 1982; Popowics and Fortelius, 1997; Steuer et al., 2010). In the first phase (the cutting phase), the sharp edge of the ectoloph interacts only with the dorsal buccal edge of the lower teeth, producing the primary tearing of

**TABLE 13.** Morphological comparison of the navicular bone of *Stephanorhinus kirchbergensis* versus *Coelodonta antiquitatis*.

	<i>Stephanorhinus kirchbergensis</i>	<i>Coelodonta antiquitatis</i>
1.	The proximal articular surface has a wide notch in the latero-plantar side.	The notch is either very weak or absent.
2.	The dorso-lateral angle is not very acute and only slightly elongated. Correlatively with this, the width of the proximal articular surface is approximately the same as the length.	The dorso-lateral angle always well pronounced and markedly elongated in the lateral direction. The proximal articular surface is more extended latero-medially.
3.	The process talocaudalis (which is used for connection with a cubic bone) is displaced to the plantar edge of the lateral side.	The process talocaudalis is placed at the middle of the lateral side.
4.	The dorso-medial angle has a convex shape.	The dorso-medial angle is oblique.
5.	The joint, on the distal side, has a well pronounced indentation in the proximal direction between facets for connection with III cuneiform and I cuneiform.	This indentation is no such pronounced.
6.	The III cuneiform facet has a well pronounced gap from the dorso-lateral edge of the bone.	This gap is no such pronounced.



**FIGURE 23.** *Stephanorhinus kirchbergensis*; Chumysh River at Kytmanovo (Kytmanovo District, Altay Territory, southeast Western Siberia). The left Mt II, NSMML-101. 1, dorsal view. 2, lateral view. 3, plantar view. 4, proximal view. The left Mt IV, NSMML-105. 5, dorsal view. 6, medial view. 7, plantar view. 8, proximal view. Scale bar ruled in centimeters.

the plant tissues. In this stage, a brief but intense stress concentrated on a small area of surface is produced. Only the serrated edge of the ectoloph participates in this phase. The shape of the ectoloph curves follows the shape of curves in lophids of the lower teeth and the dorsal buccal edge of lophids in the lower teeth. This leads to the occurrence of polished facets on the buccal edge of lophids, which are at an acute angle to the occlusal surface (Figure 24.1). In the second phase (the crushing phase), there is an interaction of the main part of the occlusal surface for both upper and lower teeth, with a translocation in the oral-aboral direction (Figure 24.5). The features of this masticatory apparatus in *Stephanorhinus kirchbergensis* were developed from a juvenile age. A characteristic facet is observed on the milk teeth of the juvenile mandible NSMML-12 (Figure 2). In brachyodont teeth, both phases are well developed, while in hypsodont teeth, the first phase is rudimentary and the second phase proves to be the main one, representing the crushing under high pressure and large side amplitude. As a result, the

occlusal surface of the upper and lower teeth of *Coelodonta antiquitatis* is flat (Figure 24.2, 24.4, 24.6).

The next adaptations are caused by different chewing forces for brachyodont and hypsodont types of teeth. A large proportion of herbaceous plants in the diet of *Coelodonta antiquitatis* increases the force required for its milling. Mandibles of large herbivores are forced to move laterally with a large amplitude, when the animal is required to create a maximum force to break the plant tissue, which has in its structure long, longitudinal, durable, and elastic fibers (as in grass). If the feeding objects have a mosaic structure, as does the leaf of a shrub or young tree, movements back and forth are enough to break it (Sanson, 2006). The increase in forces in herbivores is reached by relevant morphological adaptations of the mandible. In this case, the relative height and thickness of the horizontal corpus and the relative height of the mandibular condyle above the level of the tooth row are increased. All of the mandibles studied appear more slender than *C. antiquitatis* according

**TABLE 14.** Measurements of MtlI of *Stephanorhinus kirchbergensis* and *Coelodonta antiquitatis* from southeastern Western Siberia and Europe. All measurements are in mm. Sample sizes are given in parentheses. The following measurements were used: maximum length in the sagittal plane (ML); antero-posterior diameter of the proximal epiphysis (APD); transverse diameter of the proximal epiphysis (TD); antero-posterior diameter of the distal epiphysis (APDde); transverse diameter of the distal epiphysis (TDde); transverse diameter of the diaphysis in the middle (mTDd).

Dimensions	<i>S. kirchbergensis</i>			<i>C. antiquitatis</i>			
	Altay Territory, NSMML-101	Europe (Guérin, 1980 tab. 152)		Europe (Guérin, 1980 tab. 152)		Altay Territory and Novosibirsk Province, IAE: Krasniy Yar, Taradanovo, Chumysh	
		Range	Mean	Range	Mean	Range	Mean
ML	188	173.5 - 195	180.7(7)	140 - 157.5	148.5(37)	130.5 - 176.8	146.9(16)
APD	43.5	44 - 51	47.1(9)	36.5 - 51	41.8(34)	37 - 51.6	43(16)
TD	34	31 - 39	34.8(9)	27.5 - 38	32.6(36)	25.6 - 39.3	32.6(16)
APDde	46	41 - 48.5	43.2(7)	33.5 - 43	38.1(33)	34.7 - 46.7	37.7(16)
TDde	41	38 - 44	41(6)	31.5 - 44.5	37.6(36)	30 - 47.5	36.4(16)
mTDd	31	26.5 - 33.5	29.1(7)	23.5 - 37	31.1(37)	25.5 - 33.8	29.3(16)
Indexes, %							
TD/ML	18.1		19.2(7)		21.8(36)	17.7 - 27.1	22.3(16)
mTDd/ML	16.5		16.1(7)		20.9(37)	18.6 - 22.5	20(16)
TDde/ML	21.8		22.7(6)		25.3(36)	22.4 - 27.7	24.8(16)

**TABLE 15.** Measurements of MtlV of *Stephanorhinus kirchbergensis* and *Coelodonta antiquitatis* from southeastern Western Siberia and Europe. All measurements are in mm. Sample sizes are given in parentheses. The following measurements were used: maximum length in the sagittal plane (ML); antero-posterior diameter of the proximal epiphysis (APD); transverse diameter of the proximal epiphysis (TD); antero-posterior diameter of the distal epiphysis (APDde); transverse diameter of the distal epiphysis (TDde); transverse diameter of the diaphysis in the middle (mTDd).

Dimensions	<i>S. kirchbergensis</i>			<i>C. antiquitatis</i>				
	Altay Territory, NSMML-105	Novosibirsk Province, IAE TRD-2	Europe (Guérin, 1980 tab. 154)		Europe (Guérin, 1980 tab. 154)		Altay Territory and Novosibirsk Province, IAE: Krasniy Yar, Taradanovo, Chumysh	
			Range	Mean	Range	Mean	Range	Mean
ML	188.5	176	170 - 182.5	178.2(3)	127 - 155	144.9(40)	122.2 - 163	146.8(15)
APD	54.5	51.5	44 - 53	47.2(6)	37 - 51.5	44.3(39)	37.1 - 51.5	46.3(15)
TD	54	53	47 - 53.5	50.1(6)	41 - 57	46.5(37)	36.7 - 52.5	46.4(15)
APDde	52	46.5	44.5 - 51.5	48.8(3)	36 - 46	40.8(35)	36.3 - 47	42.5(15)
TDde	43	40	37 - 43	40.3(4)	31 - 41	36.1(36)	29.1 - 45	36.1(15)
mTDd	35	28.5	33.5 - 36.5	34.8(4)	24 - 40	30.5(40)	22.2 - 41	30.6(15)
Indexes, %								
TD/ML	28.6	30.1		28.1(3)		32.1(37)	27.1 - 37.5	31.7(15)
mTDd/ML	18.6	16.2		19.5(3)		21.1(40)	16.1 - 26.4	20.8(15)
TDde/ML	22.8	22.7		22.6(3)		24.9(36)	22.2 - 27.6	24.6(15)

to characteristics listed above. It can be seen on Figure 25, where indices of molars relative length (Figure 25; Ind. 1), horizontal corpus relative height (Figure 25; Ind. 2-7) and thickness (Figure 25; Ind. 8-12) for *S. kirchbergensis* are lower than those for *C. antiquitatis*.

The adaptation to a more selective manner of feeding is presented by a very narrow, spoon-like mandibular symphysis area and shortened viscerocranium, because of the reduced diastema (Table 4, Figure 3, Figure 8.1, occlusal view). In *Coelodonta antiquitatis*, the area of mandibular sym-

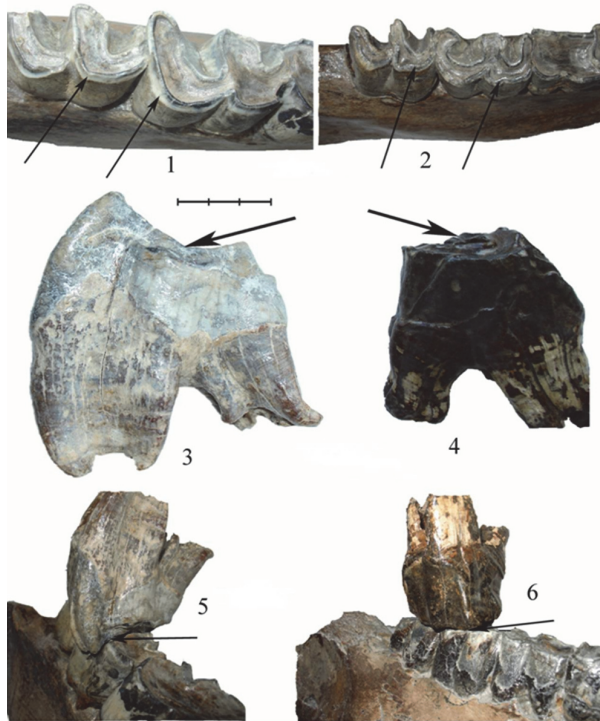


**FIGURE 24.** The specifics of the wear of the occlusal surfaces of the lower and upper teeth of *Stephanorhinus kirchbergensis* (1,3,5) and *Coelodonta antiquitatis* (2,4,6). Arrows indicate the morphological differences associated with a different biomechanical masticatory system for the browser and the grazer. Scale bar ruled in centimeters.

physis is flat, wide, and relatively long (Table 4). Another result of this adaptation may be a less wide opening of the mouth. In *Stephanorhinus kirchbergensis*, this is caused by the more acute angle of rise in the vertical ramus of the mandible (Figures 7, 10). In *C. antiquitatis*, the vertical ramus rises slightly, which allows the mouth to open wider. Another adaptation to a more selective manner of feeding could be the high body position and slender structure of the *S. kirchbergensis* postcranium. This is well illustrated by the morphometric data of the material presented (Tables 6, 7, 8, 9, 10, 11, 12, 13, 14, 15, Figures 16, 17, 18, 19, 20, 21, 22, 23). The structure of the occipital region of the cranium allowed feeding on the vegetation at a higher level. Distinctive features of *C. antiquitatis* are the adaptations for gathering food from the ground: shortened limbs, a strongly overhanging occipital crest that prevents lifting the head high, and an elongated viscerocranium caused by the shifting of orbits in the caudal direction.

### MESOWEAR ANALYSIS

Characteristics of 12 teeth of *Stephanorhinus kirchbergensis* were used as an input data for mesowear analysis. Ten of them were characterized in the present work, and data about two teeth (P4 and M1) were taken from the article of Shpan-sky and Billia (2012) (Table 16).

All of the studied upper molars of *Stephanorhinus kirchbergensis* from West Siberia had a high occlusal relief. A high percentage of teeth

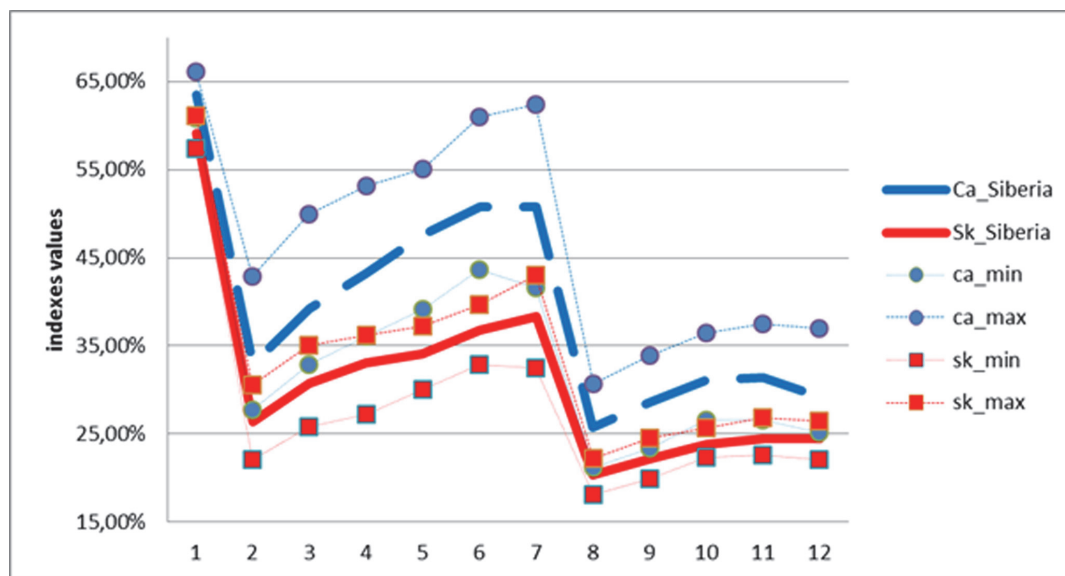


**FIGURE 25.** Indexes of the mandible of *Stephanorhinus kirchbergensis* and *Coelodonta antiquitatis*.

**TABLE 16.** Mesowear scores for occlusal relief and cusp shape for maxillary teeth of fossils *Stephanorhinus kirchbergensis* and *Coelodonta antiquitatis*.

Species	locality	Specimen identification number	Upper tooth	occlusal relief	cusp shape
				(high=h, low=l)	(sharp=s, round=r, blunt=b)
<i>Stephanorhinus kirchbergensis</i>	fossils from the southeast of Western Siberia	IAE CHU-1	M2	h	R
		IAE CHU-5	M2	h	S
		IAE CHU-2	P4	h	S
		IAE CHU-6	P4	h	S
		IAE CHU-7	P4	h	S
		IAE CHU-8	P4	h	R
		IAE BB-1	M3	h	R
		IAE CHU-4	M3	h	R
		PM TSU 5/3495	M1	h	R
		PM TSU 5/2878	P4	h	R
		PM TSU 5/396	M1	h	R
		NSMLL 21052	M2	h	S
		<i>Coelodonta antiquitatis</i>		IAE CHU 51	P4
IAE CHU 52	P4			l	R
IAE CHU 53	P4			l	R
IAE CHU 54	P4			l	B
IAE CHU 55	P4			l	R
IAE CHU 56	M1			l	B
IAE CHU 57	M1			l	R
IAE CHU 58	M1			l	B
IAE CHU 59	M1			l	B
IAE CHU 60	M1			l	B
IAE CHU 61	M1			l	R
IAE CHU 62	M2			l	R
IAE CHU 63	M2			l	R
IAE CHU 64	M2			h	R
IAE CHU 65	M2			h	R
IAE CHU 66	M2			l	R
IAE CHU 67	M2			h	R
IAE CHU 68	M2			l	B
IAE CHU 69	M2			l	R
IAE CHU 70	M2			l	R
IAE CHU 71	M3			l	B
IAE CHU 72	M3			h	R
IAE CHU 73	M3			h	R
IAE CHU 74	M3	h	R		
IAE CHU 75	M3	h	R		

have sharp apices (41.6%). The rest of the teeth have rounded apices, none of them have blunt apices (Table 17). In *C. antiquitatis* from the same region, only 28% had a high occlusal relief, 64% of specimens had rounded cusps, and 36% had blunt

cusps; no specimen displayed sharp cusps (Table 17).

Even the conservative assessment of hypsodont index (on lower third molars from the material presented) gives values close to 1.7 for *Stepha-*

**TABLE 17.** Mesowear scores for the set of 27 typical extant species and for the fossil assemblages. (Continued on next page.)

Species	Locality	Sources	label	% high	% sharp	% round	% blunt	N
<i>Stephanorhinus kirchbergensis</i>	fossils from the southeastern Western Siberia		SK_SWS	100	41,6	58,4	0	12
<i>Coelodonta antiquitatis</i>			CA_SWS	28	0	64	36	25
<i>Stephanorhinus hundsheimensis</i>	fossils from the Sussenborn	(Kahlke and Kaiser, 2011)	SH_SUES S	91.9	5.7	94.3	0	36
<i>Stephanorhinus hundsheimensis</i>	fossils from the Voigtstedt		SH_VOI	100	100	0	0	6
<i>Stephanorhinus hemitoechus</i>	fossils from the Bilzingsleben II	(Asperen and Kahlke, 2014)	SHM_B	80	12	88	0	25
<i>Stephanorhinus kirchbergensis</i>			SK_B	82.6	8.7	87	4.3	23
<i>Stephanorhinus kirchbergensis</i>	fossils from the Weimar-Ehringsdorf		SK_WE	89.5	28.9	71.1	0	76
<i>Stephanorhinus kirchbergensis</i>	fossils from the Weimar-Taubach		SK_WT	82.6	39.1	60.9	0	23
<i>Stephanorhinus hemitoechus</i>	fossils from the UK MIS 7		SHM_U7	36.4	30	60	10	11
<i>Stephanorhinus kirchbergensis</i>			SK_U7	83.3	16.7	66.7	16.6	6
<i>Stephanorhinus hemitoechus</i>	fossils from the UK MIS 5e upland		SHM_U5u	85.7	9.5	90.5	0	21
<i>Stephanorhinus hemitoechus</i>	fossils from the UK MIS 5e lowland		SHM_U5l	63.6	9.1	81.8	9.1	11

*norhinus kirchbergensis* from West Siberia and 2 or a little larger for *Coelodonta antiquitatis*. Thus, *S. kirchbergensis* can be classified as brachyodont type, while *C. antiquitatis* belongs to the mesodont type. But, as shown in by Fortelius and Solounias (2000), using only the hypsodont index does not allow classifying definitely the individuals. In addition, this characteristic affects slightly the results of mesowear analysis.

Two groups of attributes of dental specimens were used as an input for a Mann-Whitney U-test: one for *Stephanorhinus kirchbergensis* and the other for *Coelodonta antiquitatis*. The values of attributes were formed based on two mesowear variables (relief of the occlusal surface and the shape of cusps) listed in Table 16, as follows: 1 = high and sharp; 2 = high and rounded; 3 = low and sharp; 4 = low and rounded; and 5 = low and blunt. The test result showed the expected high degree of difference between *S. kirchbergensis* and *C. antiquitatis* in dietary mesowear signals, i.e., the probability of the coincidence of these two groups was negligible ( $p < 0.001$ ).

The diagram summarizing the cluster analysis (Figure 26) reflects the distribution of the fossil rhi-

noceroses of Europe and Siberia according to dietary preferences, against the reference data set of 27 species of extant ungulate mammals selected by Fortelius and Solounias (2000) on the basis of information about their dietary preferences (Janis, 1988). The distribution of these 27 extant ungulates in the diagram completely coincides with other lines of paleodietary evidence (Fortelius and Solounias 2000; Kaiser and Solounias, 2003; Kahlke and Kaiser, 2011). The distribution of European *S. hundsheimensis* in the diagram is congruent with data from Kahlke and Kaiser (2011), and distributions of *Stephanorhinus kirchbergensis* and *S. hemitoechus* are congruent with data from van Asperen and Kahlke (2014). The diagram illustrates the partition of the set of the animals examined into four groups. The extreme groups are grazers and browsers. The browsers group includes animals whose diet comprises no more than 10% of grass. The grazers group includes animals whose diet is more than 90% of grass. Animals with a mixed diet are placed in the central part of the diagram. The group that is closer to the grazers consists of the mixed grazer feeders with prevailing consumption of grass, compared to another

TABLE 17 (continued).

Species	Locality	Sources	label	% high	% sharp	% round	% blunt	N
<i>Alces alces</i>	extant species	(Fortelius and Solounias, 2000)	AA	100	100	0	0	30
<i>Diceros bicornis</i>			DB	100	94.1	5.9	0	34
<i>Dicerorhinus sumatrensis</i>			DS	100	80	20	0	5
<i>Giraffa camelopardalis</i>			GC	94	73.7	26.3	0	61
<i>Odocoileus hemionus</i>			OH	100	72.7	27.3	0	33
<i>Odocoileus virginianus</i>			OV	100	88.8	11.2	0	18
<i>Okapia johnstoni</i>			OJ	100	87.5	12.5	0	8
<i>Rhinoceros sondaicus</i>			RS	100	100	0	0	5
<i>Ceratotherium simum</i>			cs	0	0	72	28	26
<i>Alcelaphus buselaphus</i>			ab	57	4.4	67.6	28	76
<i>Bison bison</i>			bb	0	0	26.7	73.3	15
<i>Connochaetes taurinus</i>			ct	55	15.3	55.7	29	52
<i>Damaliscus lunatus</i>			dl	20	20	60	20	5
<i>Equus burchelli</i>			eb	0	27	39.4	33.6	122
<i>Equus grevyi</i>			eg	0	34.4	41.4	24.2	29
<i>Hippotragus equinus</i>			he	85	3.9	96.1	0	26
<i>Hippotragus niger</i>			hn	85	0	85	15	20
<i>Kobus ellipsiprymnus</i>			ke	96	0	100	0	22
<i>Redunca redunca</i>			rr	91	6.4	91	2.6	77
<i>Aepyceros melampus</i>			Me	100	35.3	64.7	0	17
<i>Capricornis sumatraensis</i>			Ca	100	45.5	50	4.5	22
<i>Cervus elaphus canadensis</i>			Cc	100	47.4	52.6	0	19
<i>Gazella granti</i>			Gg	88	50	50	0	18
<i>Gazella thomsoni</i>			Gt	88	55.5	43.2	1.3	146
<i>Ovibos moschatus</i>			Om	81	57.6	42.4	0	52
<i>Taurotragus oryx</i>			To	100	50	50	0	14
<i>Tragelaphus scriptus</i>			Ts	100	51	49	0	47

central group that is closer to the browsers, which is mixed browser feeders.

The position of West Siberian *Coelodonta antiquitatis* in the diagram lies adjacent to the typical extant grazer *Ceratotherium simum*. This is due to very similar values of mesowear signals of these two species of rhino, indicating the same high level of adaptation to the rough abrasive food base. *Stephanorhinus kirchbergensis* of West Siberia appears in the same group with extant mammals such as the impala (*Aepyceros melampus*), suma-

tran serow (*Capricornis sumatraensis*), wapiti (*Cervus elaphus canadensis*), Grant's gazelle (*Gazella granti*), Thomson's gazelle (*Gazella thomsoni*), (*Ovibos moschatus*), common eland (*Taurotragus oryx*), and bushbuck (*Tragelaphus scriptus*). This group of animals belongs to mixed browser feeders. It is caused by a small Euclidean distance between the mesowear signals of animals from this group. Also, specimens of *S. kirchbergensis* from the beginning of the Late Pleistocene in the European areas of Weimar-Ehringsdorf and Weimar-

## Cluster Tree

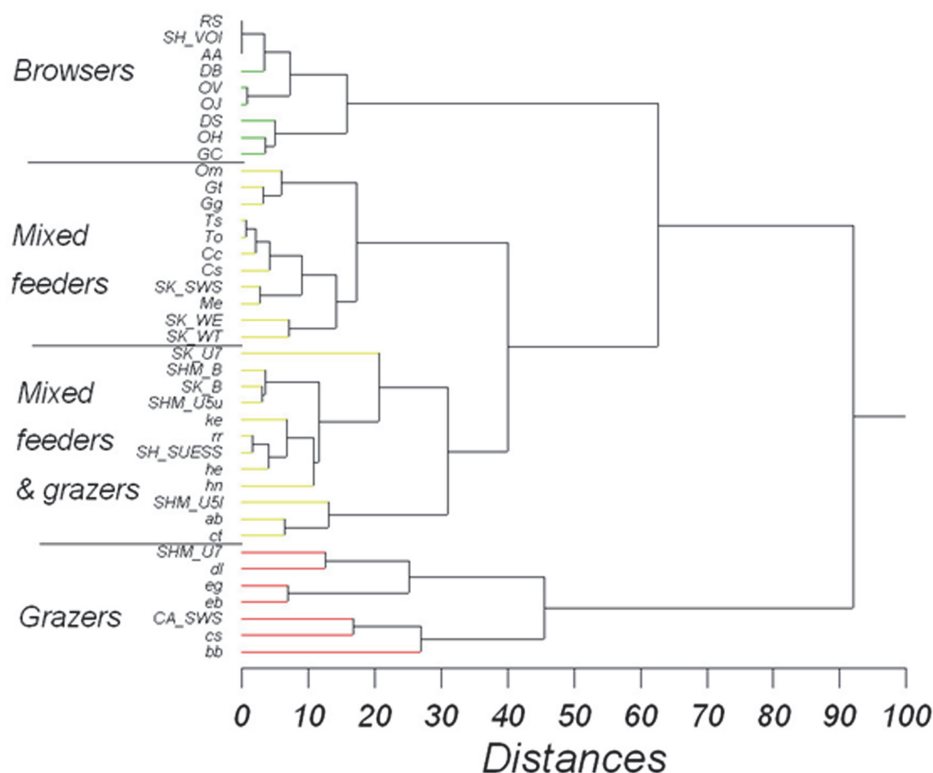


**FIGURE 26.** Hierarchical cluster diagram based on the reference tooth positions of upper P4-M3 according to the extended mesowear method (Kaiser and Solounias, 2003). Distances = Euclidean distance (root-mean-squared difference). Clusters are based on a set of 27 typical extant species model. Classification follows the conservative (CONS) scheme of Fortelius and Solounias (2000): Browsers (CONS): AA = *Alces alces*, DB = *Diceros bicornis*, DS = *Dicerorhinus sumatrensis*, GC = *Giraffa camelopardalis*, OH = *Odocoileus hemionus*, OJ = *Okapia johnstoni*, OV = *Odocoileus virginianus*, RS = *Rhinoceros sondaicus*, Grazers (CONS): ab = *Alcelaphus buselaphus*, bb = *Bison bison*, cs = *Ceratotherium simum*, ct = *Connochaetes taurinus*, dl = *Damaliscus lunatus*, eb = *Equus burchelli*, eg = *Equus grevyi*, he = *Hippotragus equinus*, hn = *Hippotragus niger*, ke = *Kobus ellipsiprymnus*, rr = *Redunca redunca*; Mixed feeders (CONS): Cc = *Cervus elaphus canadensis*, Ca = *Capricornis sumatraensis*, Gg = *Gazella granti*, Gt = *Gazella thomsoni*, Me = *Aepyceros melampus*, Om = *Ovibos moschatus*, To = *Taurotragus oryx*, Ts = *Tragelaphus scriptus*. European fossil populations of *Stephanorhinus hundsheimensis* (Kahlke and Kaiser, 2011): SH\_SUESS = Su  $\bar{\text{B}}$ enborn, SH\_VOI = Voigtstedt; *S. kirchbergensis* (van Asperen and Kahlke, 2014): SK\_B = Bilzingsleben II, SK\_WE = Weimar-Ehringsdorf, SK\_WT = Weimar-Taubach, SK\_U7 = UK MIS 7; *S. hemitoechus* (van Asperen and Kahlke, 2014): SHM\_B = Bilzingsleben II, SHM\_U7 = UK MIS 7, SHM\_U5u = UK MIS 5e upland, SHM\_U5l = UK MIS 5e lowland. Southeast Western Siberia fossil populations: SK\_SWS = *S. kirchbergensis*, CA\_SWS = *Coelodonta antiquitatis*.

Taubach also belong to this group (van Asperen and Kahlke, 2014).

### BIOGEOCHEMICAL ANALYSES

To date, a great deal of information is known about the biogeochemistry of Quaternary mammal remains and particularly about rhinos. But research on the *Stephanorhinus* genus is rare (Palmqvist et

al., 2003), and even less information is presented specifically on *S. kirchbergensis* (Pushkina et al., 2014). Comparative study of the biogeochemical composition (including stable isotopes) of bone tissue was made for the Sk\_ui1 sample and a number of samples of Late and Middle Pleistocene mammals from Middle Irtysh and other regions because of uncertainty about the findings' age (probably Middle Pleistocene). We have estab-

lished that the amount of trace elements in the Sk\_ui1 tissue sample from the Ust-Ishim area (0.2 mass %) falls into the same group with suspected or known Late Pleistocene remnants (0.1–0.25 mass %) and is significantly different from those of the Middle Pleistocene (0.35–0.4 mass %). The Sk\_ui1 sample also displayed a quite large organic carbon content (11.42 mass %), typical for Late Pleistocene samples. The stable isotopic analysis of Sk\_ui1 gave the following results: 1) for bone bioapatite,  $\delta^{13}\text{C}_{\text{PDB}} = -11.30\text{‰}$ ; and 2) for bone collagen,  $\delta^{13}\text{C}_{\text{PDB}} = -19.66\text{‰}$ ,  $\delta^{15}\text{N}_{\text{air}} = 2.84\text{‰}$ . The stable isotopic composition of the bone sample of a woolly rhinoceros from Ust-Ishim region was: 1) for bone bioapatite,  $\delta^{13}\text{C}_{\text{PDB}} = -9.40\text{‰}$ ; and 2) for bone collagen,  $\delta^{13}\text{C}_{\text{PDB}} = -19.33\text{‰}$ ,  $\delta^{15}\text{N}_{\text{air}} = 5.40\text{‰}$ . Parameters of mammalian tissues' stable isotopic composition are determined by isotope fractionation in the food and water, which changes naturally through the food chains from the producers with a different type of photosynthesis and preferred habitats to consumers of higher trophic levels (Bocherens and Drucker, 2013). Interpreting the stable isotopic composition of the tissues is more effective when there is complex evidence for several species and many specimens of each species, because individual values vary, and the total ensemble of data may be shifted in isotopic values depending on the geochemical and climatic conditions of the region (Bocherens, 2003). However, the interpretation of individual measurements is also possible by using the accumulated information. The degree of enrichment of collagen by  $\delta^{15}\text{N}$  isotope is very informative. Low values of  $\delta^{15}\text{N}$  in collagen of herbivores can be explained by several factors: the use of food that is pioneer vegetation, increased acidity of soils, and the predominance of shrubs and trees in the diet spectrum (Bocherens, 2003). This is in agreement with the traditional view about the browsing feeding strategy of *S. kirchbergensis* and the mesowear analysis results for Siberian specimens. For instance, significantly reduced  $\delta^{15}\text{N}$  relative values are characteristic of browsers such as *Alces alces*, *Cervus elaphus*, and *Rangifer tarandus*. The value of  $\delta^{15}\text{N}$  for Sk\_ui1 is smaller than that for the woolly rhinoceros from Belgium, France, and Yakutia (Bocherens, 2015), while the comparative sample of woolly rhinoceros from the Irtysh Valley corresponds to the values for European representatives of this species. This discrepancy may reflect different nutritional adaptation of two species of Siberian rhinoceroses. High  $\delta^{13}\text{C}$  value (as in both

test samples) is characteristic for inhabitants of open ecosystems where there are dominant plants with  $\text{C}_3$  type of photosynthesis and/or an abundance of lichens in the vegetation cover. The stable isotopic composition of bioapatite of both *S. kirchbergensis* and *C. antiquitatis* suggests that they consumed very fresh, probably largely melt, water.

### MORPHOMETRIC ANALYSIS OF THE JUVENILE MANDIBLE

At present, juvenile mandibles of *Stephanorhinus kirchbergensis* are known in several localities in Europe, China (Shennongjia) (Kahlke, 1975, 1977; Guérin, 1980; Lacombat, 2006; Tong and Wu, 2010), and Altai (Russia) (NSMLL-12). The largest number of juvenile mandibles is known in the localities of Weimar-Taubach and Weimar-Ehringsdorf in Europe. A representative collection of *Coelodonta antiquitatis* juvenile mandibles of different individual ages from the following localities was used as comparative material: Krasniy Yar of Tomsk Province (Shpansky, 2014), Novosibirsk Province, and Altai Territory.

The main differences between juvenile mandibles of *S. kirchbergensis* and those of *Coelodonta antiquitatis* are the absence of thickening in the ventral part of the horizontal corpus and more massive teeth (Table 2).

The change in the average indices of lower deciduous teeth (relation of tooth width to its length) from dp1 to dp4 is not linear in *Stephanorhinus kirchbergensis* or in *Coelodonta antiquitatis* (Figure 27). At the same time, the main trend in *C. antiquitatis* from West Siberia is that the greatest width index is observed on dp2, while dp4 has less width index than dp2, and it has often the minimal value of width index with respect to the other teeth of the same jaw (Figure 28). Dynamics of changes in the average values of the width indices of the deciduous teeth from dp1 to dp4 in *C. antiquitatis* from West Siberia, as well as from European regions, reflects this general trend. The exception is the value for dp1 in the European plot, which was obtained from the only specimen, and therefore may not reflect the value of the population (Figure 27). For the mandible of *S. kirchbergensis* (NSMLL-12), another index distribution is observed. The width index of dp4 is the highest. It is much greater than the width index of dp2 (Figure 29). The same may be observed for four mandibles from Weimar-Taubach (MIS 5e) (Kahlke, 1977), where the width index of all dp4 is at least the same as that of dp2 (Figure 29). For the older locality of Weimar-Ehringsdorf (MIS 7) (Kahlke,

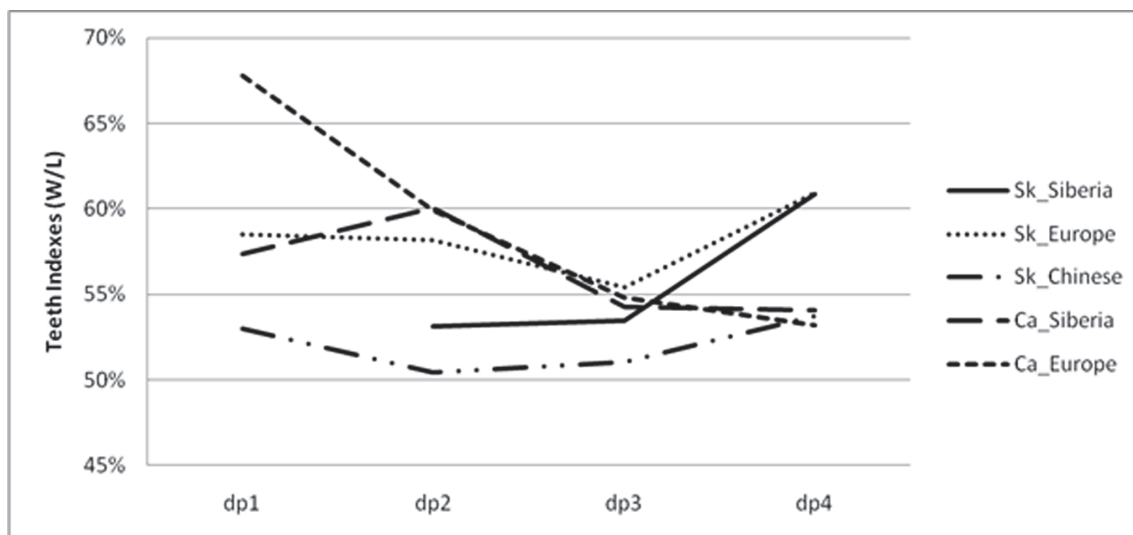


**FIGURE 27.** Indexes of the lower deciduous teeth of *Stephanorhinus kirchbergensis* and *Coelodonta antiquitatis* from Siberian, European, and Chinese regions.

1975), the width index of dp4 compared to dp2 is more variable. The maximal value of the width index is observed on dp1, but the main trend in the width index of dp4 and dp2 remains the same, i.e., for three of five jaws that we present here, the width index of dp4 is lower than that of dp2. In the other two jaws, the width index between dp4 and dp2 is close to that in *C. antiquitatis* (Figure 29). Considering that mesowear signals of adults from the locality of Weimar-Ehringsdorf (MIS 7) on the hierarchical graph (Figure 26) also shift towards grazers, the slight shift of teeth proportions in juveniles towards the *C. antiquitatis* condition appears quite explainable. The trend of changes in deciduous teeth indices from dp1 to dp4 in NSMML-12 is similar with the trend of change in the indices of *S. kirchbergensis* average indices from Europe (Figure 27). For localities in China, we can only observe the general dynamics of the average indices of the deciduous teeth from dp1 to dp4 for *S. kirchbergensis* (Figure 27), because Tong and Wu (2010) provided information only on isolated teeth and there is no full information on mandibles of juveniles.

To determine the age of the juvenile NSMML-12, a juvenile individuals of extant African black rhinos (*Diceros bicornis*) and white rhinos (*Ceratotherium simum*) were used as comparative material (Schaurte, 1966; Dittrich, 1974), and the method of age determination proposed by Hillman-Smith et al. (1986) was used. Based on the assumption that the order of deciduous teeth eruption, functioning, and replacement were close to those of extant rhinoceroses, we applied the method introduced by

Hillman-Smith et al. (1986) in order to estimate the age of NSMML-12. In NSMML-12, only the deciduous teeth dp2 (STL5), dp3 (STL5), and dp4 (STL4) were erupted and functioned in the initial stage. The degree of wear of preserved deciduous teeth of NSMML-12 is closest to the specimen IQW 1968/9761 of the juvenile mandible of *S. kirchbergensis* from Taubach (Kahlke, 1977). Therefore, dp1 in NSMML-12 was not used, or dp1 was used in the earliest stage (STL2 or STL3), just as in IQW 1968/9761. Because alveolar pockets for permanent teeth P2 and P3 were not found after apertum of the NSMML-12 textus, it is likely that m1 had not yet started erupting from the bone tissue. It corresponds to stages STL1 or STL2. Information about stages of wear of dp1-m1 from NSMML-12 completely corresponds to information on the expected state of mandibular teeth in Hillman-Smith et al. (1986: table IV). This corresponds to the age of a juvenile rhinoceros, 12–18 months.

## DISCUSSION

Sizes and morphological features of lower dentitions and mandibles from different locations in Siberia correspond to specimens known from Europe. The adult mandibles studied may be separated into two groups, which differ considerably by the length of their tooth rows. The first group, including the specimens IAE KY-4323, IRM 2436, and GR PC 1165, is characterized by the length of p2-m3 varying from 263 mm to 265 mm. The second group of specimens, NSMML-10, Sk\_ui1, NSMML 22090, GR PC 1164, and KB MAN K-397, has a length of tooth row that varies from 278 mm

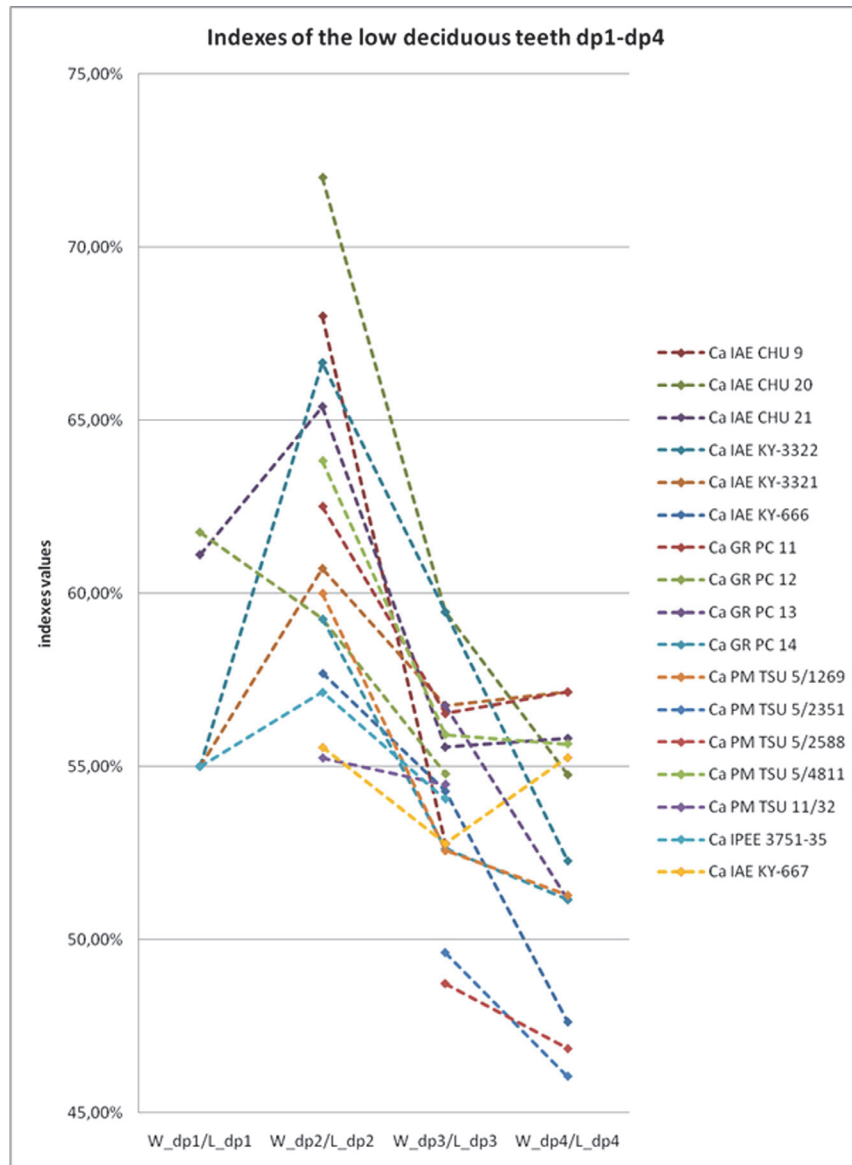


**FIGURE 28.** Indexes of the lower deciduous teeth dp1-dp4 of *Coelodonta antiquitatis* (Ca).

to 289 mm. Premolar tooth row p2-4 length for all mandibles varies from 108 mm to 118 mm (Table 4). Differences are more visible in the length of m1-3. For the first group, the length of m1-3 varies from 152 mm to 155 mm, while for the second it varies from 163 mm to 171 mm. It may be assumed that these differences are a consequence of expressed sexual dimorphism of body size for *Stephanorhinus kirchbergensis*, by analogy with sexual dimorphism of body size in extant species: *Rhinoceros unicornis* (Dinerstein, 1991) and *Ceratottherium simum* (Owen-Smith, 1975). Thus, of the total number of jaws considered, 30% are jaws with short dentition (presumably female), 20% are

young individuals (less than 10 years old), and 50% are jaws with a long dentition (presumably male). All jaws with a short tooth row belong to adult animals older than 20 years, while there are two groups for the jaws with a long dentition: young animals aged 15–20 years and individuals over 20 years old. To a certain extent this distribution agrees with the general model of sexual dimorphism of extant rhinos that reflects the hierarchy of dominance (Mihlbachler, 2003, 2005, 2007). This model explains the resurgence in mortality among young rhino males because of the severe dominance of older individuals. Such a surge in mortality is not observed among females. A more detailed

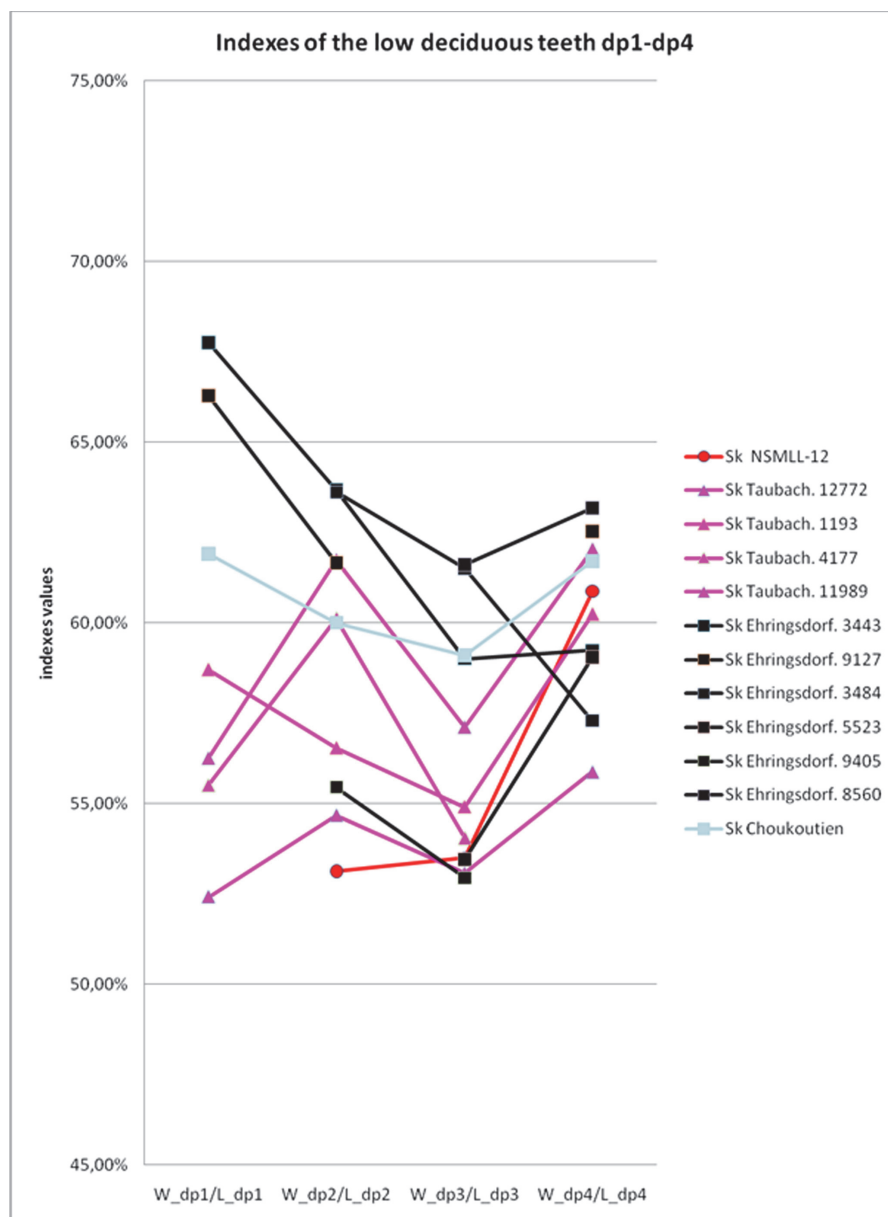


**FIGURE 29.** Indexes of the lower deciduous teeth dp1-dp4 of *Stephanorhinus kirchbergensis* (Sk).

study of the model of sexual dimorphism of *S. kirchbergensis* using the capabilities of statistical systems is currently impossible because of the insufficient amount of material. For the same reason, it has been impossible to study the morphology of sexual dimorphism, because for definitive studies it is necessary to have complete skeletons of *S. kirchbergensis* individuals of both sexes, or at least complete skulls with mandibles, which to date have not been found.

Comparative analysis of the postcranium from the localities of West Siberia showed their morpho-

logical similarity and closeness in size to remains of *Stephanorhinus kirchbergensis* from Europe.

Morphological analysis of the dental features presented and comparison with extant typical browsers and grazers (Fortelius, 1982; Clauss et al., 2008) show the shift towards the browsers in the material studied. On the other hand, it would be an oversimplification to assume that *Stephanorhinus kirchbergensis* was exclusively a forest dweller. The diet of *S. kirchbergensis* contained a high percentage of abrasive food, as is observed from mesowear analysis of European remains (Hernesniemi et al., 2011; Kahlke and Kaiser, 2011;

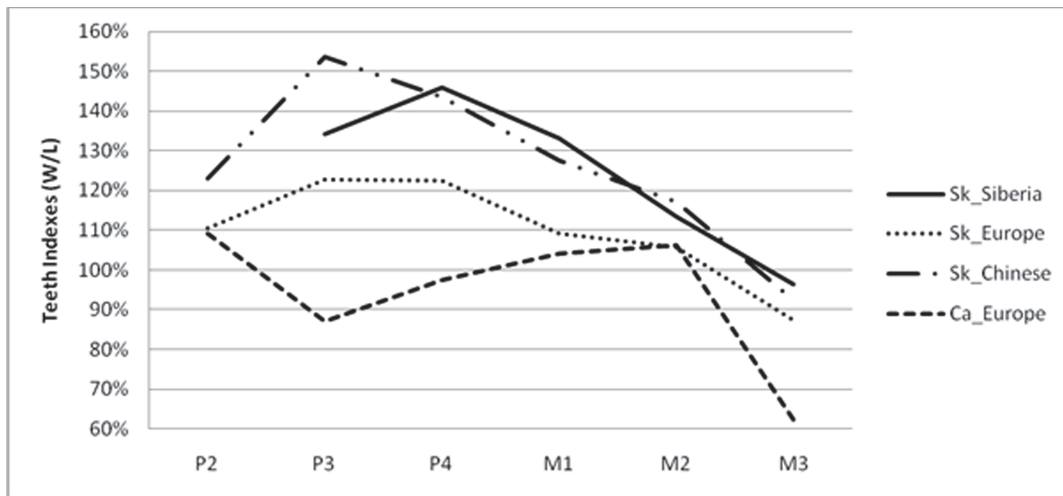


**FIGURE 30.** Indexes of the upper permanent teeth of *Stephanorhinus kirchbergensis* and *Coelodonta antiquitatis* from Siberian, European, and Chinese regions.

van Asperen and Kahlke, 2014); these analyses showed significant dietary flexibility that depended on the quality of the ecological environment. At the same time, morphological features and mesowear signals of *S. kirchbergensis* inhabiting Europe in the Late Pleistocene indicate a higher dietary specialization shifted to browsers, compared with the early and Middle Pleistocene. Mesowear analysis of the dietary preferences of Siberian *S. kirchbergensis* also shows their higher dietary specialization, comparable to mesowear signals of *S. kirchbergensis* from the beginning of the Late Pleistocene in Europe from Weimar-Taubach (van Asperen and Kahlke, 2014). However, the heavy continental climate of Siberian regions and the poorer food base contributed to the process of *S. kirchbergensis* adaptation to the local environment. In addition to the increased molar row length, characteristic of *S. kirchbergensis* in all regions of their habitat, representatives of the Siberian region tend to increase the relative width of the upper and lower molars (Figures 30, 31). Thus, the increase in the occlusal surface area is observed. It allowed increasing the volume of the processed food per unit of time and adapting to the poor food base. According to the results of mesowear analysis, unlike *Coelodonta antiquitatis*, *S. kirchbergensis* could not inhabit West Siberia in the periods of tundra–steppe habitat conditions. The structure and relief of the occlusal surface of teeth show that *S. kirchbergensis* had not adapted to using strongly abrasive vegetation. Even in the interglacial periods, it probably had to disperse to the more southerly areas, for the same reasons. The results of the

stable isotopic study of the single sample of the Siberian *S. kirchbergensis* indicate that it was a browser-type that fed presumably in predominantly open landscapes.

Despite overall similar mesowear signals for *Stephanorhinus kirchbergensis* in the Siberian region and in Europe at the beginning of Late Pleistocene (MIS 5e), it cannot be stated with certainty that *S. kirchbergensis* existed contemporaneously in Siberia and Europe. A variety of landscape and climatic conditions and interspecies competition had led to significant variability of Pleistocene rhinoceroses' feeding behavior (van Asperen and Kahlke, 2014). This circumstance does not allow extrapolating the paleoecological assessments gained from the European materials to Siberian representatives of *S. kirchbergensis*. On one hand, all the remains of *S. kirchbergensis* previously found in southeastern West Siberia (Kemerovo and Tomsk Provinces) (Alekseeva, 1980; Shpansky and Billia, 2012) and on Vilyuy River (Dubrovo, 1957) were assigned to the Middle Pleistocene, based on accompanying fauna, including *Mammuthus* ex gr. *trogotherii-chosari-cus*, *Megaloceros giganteus ruffi*, and *Equus* ex gr. *mosbachensis-germanicus*. In addition, it can be noted that the degree of fossilization of the existing Middle Pleistocene residues agrees to a certain extent with the degree of fossilization of new remains of *S. kirchbergensis* from the Altai Territory and Novosibirsk Province. On the other hand, although the latest findings of *S. kirchbergensis* on the beaches from Altai Territory and Novosibirsk Province do not have a stratigraphic linkage, it is

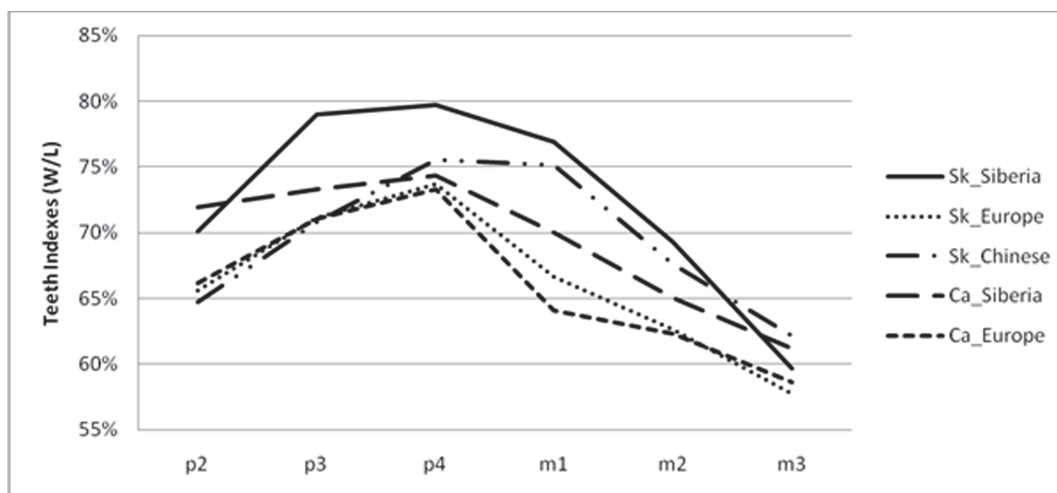


**FIGURE 31.** Indexes of the lower permanent teeth of *Stephanorhinus kirchbergensis* and *Coelodonta antiquitatis* from Siberian, European, and Chinese regions.

characteristic that the accompanying fauna of all these locations is mainly from the Late Pleistocene, and there are very few remains of the Middle Pleistocene megafauna.

However, until now, none of the finds related to *Stephanorhinus kirchbergensis* discovered in Siberia has been unequivocally attributed to the Late Pleistocene. Quantitative data on the chemical composition of the sample from the Middle Irtysh give an indirect indication that individual specimens of *S. kirchbergensis* could have existed in West Siberia in the Late Pleistocene. To date, we can assert that despite its small number, the population of *S. kirchbergensis* was distributed fairly widely in Siberia in the places most favorable to their dietary preferences—river valleys with rich bush vegetation.

## ACKNOWLEDGMENTS

The authors are thankful to E.M. Matskevich, the head of the Museum of Arts of the North Peoples (Kargasok settlement, Tomsk Province); I.V. Orlova, main curator of the Novosibirsk State Museum of Local History; V.K. Kreshik, assistant to the chief curator of Novosibirsk State Museum of Local History; I.N. Shitikova, head of the Nature Department of the Irkutsk Local History Museum; N.V. Peristov, head of the studio Arhaika; and A.L. Dorogov for access to collections of *Stephanorhinus kirchbergensis* remains. This study (research grants No 8.1.80.2015) was supported by the Tomsk State University Academic D. I. Mendeleev Fund Program in 2015. The authors thank S. Ivantsov, Tomsk State University, for translation, and J. Kollantai, Tomsk State University, for style review.

## REFERENCES

- Alekseeva, E.V. 1980. Mlekopitayushchie Pleistocena yugo-vostoka Zapadnoi Sibiri. Nauka, Moscow. [In Russian]
- Belyaeva, E.I. 1940. Novye nakhodki ostatkov nosoroga Mercka na territorii SSSR. Priroda, 8:82. [In Russian]
- Belyaeva, E.I. 1966. Semeistvo Rhinocerotidae Owen, 1845. In Mlekopitayushchie eopleistocena Zapadnogo Zabaikalia. Trudy Geologicheskogo instituta Akademii Nauk SSSR, 152:92-143. [In Russian]
- Billia, E.M.E. 2007. First records of *Stephanorhinus kirchbergensis* (Jäger, 1839) (Mammalia, Rhinocerotidae) from the Kuznetsk Basin (Kemerovo region, Kuzbass area, South-East of Western Siberia). Bollettino della Società Paleontologica Italiana, 46:95-100.

- Billia, E.M.E. 2008a. The skull of *Stephanorhinus kirchbergensis* (Jäger 1839) (Mammalia, Rhinocerotidae) from the Irkutsk region (Southwest Eastern Siberia). *Quaternary International*, 179:20-24. <https://doi.org/10.1016/j.quaint.2007.08.034>
- Billia, E.M.E. 2008b. Revision of the fossil material attributed to *Stephanorhinus kirchbergensis* (Jäger 1839) (Mammalia, Rhinocerotidae) preserved in the museum collections of the Russian Federation. *Quaternary International*, 179:25-37. <https://doi.org/10.1016/j.quaint.2007.09.034>
- Billia, E.M.E. 2011a. Siti paleontologici a "Rinoceronte di Merck", *Stephanorhinus kirchbergensis* (Jäger, 1839) (Mammalia, Perissodactyla), in Istria, Quarnero e Dalmazia [Paleontoloska Najdisca Merckovega Nosoroga, *S. kirchbergensis* (Jäger, 1839) (Mammalia, Perissodactyla) v Istri in Dalmaciji – Paleontoloska nalazista Merckovog Nosoroga, *S. kirchbergensis* (Jäger, 1839) (Mammalia, Perissodactyla), u Istri i Dalmaciji]. *Atti - Centro di Ricerche Storiche / Centar za Povijesna Istrazivanja / Sredisce za Zgodovinska Raziskovanja, Rovigno/Rovinj, Croatia/Hrvatska*, XLI:9-31. (with English, Croatian & Slovenian abstracts)
- Billia, E.M.E. 2011b. Occurrences of *Stephanorhinus kirchbergensis* (Jäger, 1839) (Mammalia, Rhinocerotidae) in Eurasia – An account. *Acta Palaeontologica Romaniae*, 7:17-40.
- Bocherens, H. 2003. Isotopic biogeochemistry and the paleoecology of the mammoth steppe fauna. *DEINSEA*, 9:57-76.
- Bocherens, H. 2015. Isotopic tracking of large carnivore palaeoecology in the mammoth steppe. *Quaternary Science Reviews*, 117:42-71. <https://doi.org/10.1016/j.quascirev.2015.03.018>
- Bocherens, H. and Drucker, D.G. 2013. Terrestrial teeth and bones, p. 304-314. In Elias, S.A. and Mock, C.J. (eds.), *Encyclopedia of Quaternary Science*. 2nd edition. Elsevier, Edinburgh. <https://doi.org/10.1016/b978-0-444-53643-3.00341-1>
- Chersky, I.D. 1874. Opisanie cherepa nosoroga, razlichnago ot' *Rhinoceros tichorhinus*. *Zapiski Imperatorskoy Akademii Nauk*, 25:65-75. [In Russian]
- Chow, B.-S. 1979. The fossil rhinocerotides of locality 1, Choukoutien. *Vertebrata Palasiatica*, 17:236-258. [In Chinese with English summary]
- Clauss, M., Kaiser, T., and Hummel, J. 2008. The morphophysiological adaptations of browsing and grazing mammals, p. 47-88. In Gordon, I.J. and Prins, H.H.T. (eds.), *The Ecology of Browsing and Grazing*. Springer, Berlin. [https://doi.org/10.1007/978-3-540-72422-3\\_3](https://doi.org/10.1007/978-3-540-72422-3_3)
- David, I.A., Tatarinov, K.A., and Svistun, V.I. 1990. Khishchnye, khobotnye i kopytne rannego Pleistocena yugo-zapada SSSR. *Shtiinca, Kishinyov*. [In Russian]
- Dinerstein, E. 1991. Sexual dimorphism in the greater one-horned rhinoceros (*Rhinoceros unicornis*). *Journal of Mammalogy*, 72:450-457. <https://doi.org/10.2307/1382127>
- Dittrich, L. 1974. Beobachtungen zum Milchzahndurchbruch beim Spitzmaul- (*Diceros bicornis*) und Breitmaulnashorn (*Ceratotherium simum*). *Säugetierkundliche Mitteilungen*, 22:289-295.
- Dubrovo, I.A. 1957. Ob ostatkakh *Parelephas wüsti* (Pawl.) i *Rhinoceros mercki* Jaeger iz Yakutii. *Bjulletin Komissii Izucheniya Chetvertichnogo Perioda*, 21:97-104. [In Russian]
- Fortelius, M. 1982. Ecological aspects of dental functional morphology in the Plio-Pleistocene rhinoceroses of Europe, p. 163-181. In Kurtén, B. (ed.), *Teeth: Form, Function, and Evolution*. Columbia University Press, New York.
- Fortelius, M., Mazza, P., and Sala, B. 1993. *Stephanorhinus* (Mammalia: Rhinocerotidae) of the western European Pleistocene, with a revision of *S. etruscus* (Falconer, 1868). *Palaeontographia Italica*, 80:63-155.
- Fortelius, M. and Solounias, N. 2000. Functional characterization of ungulate molars using the abrasion-attribution wear gradient: a new method for reconstructing paleodiets. *American Museum Novitates*, 3301:1-36. [https://doi.org/10.1206/0003-0082\(2000\)301%3C0001:fcoumu%3E2.0.co;2](https://doi.org/10.1206/0003-0082(2000)301%3C0001:fcoumu%3E2.0.co;2)
- Gromova, V.I. 1935. Ob ostatkakh nosoroga Merka (*Rhinoceros mercki* Jaeg.) s nizhnei Volgi. *Trudy Paleozoologicheskogo Instituta Akademii Nauk SSSR*, 4:91-136. [In Russian]
- Gromova, V.I. 1950. Opredelitel' mlekopitayushchikh SSSR po kostyam skeleta. *Trudy komissii po izuchenyu chetvertichnogo perioda*, 9(1):1-240. [In Russian]
- Guérin, C. 1980. Les rhinocéros (Mammalia, Perissodactyla) du Miocène terminal au Pléistocène supérieur en Europe occidentale: comparaison avec les espèces actuelles. *Documents des Laboratoires de Géologie Lyon*, 79:1-421.
- Hernesniemi, E., Blomstedt, K., and Fortelius, M. 2011. Multi-view stereo three-dimensional reconstruction of lower molars of Recent and Pleistocene rhinoceroses for mesowear analysis. *Palaeontologia Electronica*, 14.2.2T.

- Hillman-Smith, A.K.K., Owen-Smith, N., Anderson, J.L., Hall-Martin, A.J., and Selaladi, J.P. 1986. Age estimation of the white rhinoceros (*Ceratotherium simum*). *Journal of Zoology*, 210:355-379. <https://doi.org/10.1111/j.1469-7998.1986.tb03639.x>
- Hitchins, P.M. 1978. Age determination of the black rhinoceros (*Diceros bicornis* Linn.) in Zululand. *South African Journal of Wildlife Research*, 8:71-80.
- Jäger, G.F. 1835–39. Über die fossilen Säugetiere welche in Württemberg in verschiedenen Formationen aufgefunden worden sind, nebst geognostischen Bemerkungen über diese Formationen. C. Erhard Verlag, Stuttgart.
- Janis, C.M. 1988. An estimation of tooth volume and hypsodonty indices in ungulate mammals, and the correlation of these factors with dietary preferences. *Mémoires du Muséum National d'Histoire Naturelle*, 53:367-387.
- Kahlke, H.-D. 1975. Die Rhinocerotiden-Reste aus den Travertinen von Weimar-Ehringsdorf. *Palaontologische Abhandlungen*, 23:337-397.
- Kahlke, H.-D. 1977. Die Rhinocerotidenreste aus den Travertinen von Taubach. *Quartärpaläontologie*, 2:305-359.
- Kahlke, R.-D. and Kaiser, T.M. 2011. Generalism as a subsistence strategy: advantages and limitations of the highly flexible feeding traits of Pleistocene *Stephanorhinus hundsheimensis* (Rhinocerotidae, Mammalia). *Quaternary Science Reviews*, 30:2250-2261. <https://doi.org/10.1016/j.quascirev.2009.12.012>
- Kaiser, T.M. and Solounias, N. 2003. Extending the tooth mesowear method to extinct and extant equids. *Geodiversitas*, 25:321-345.
- Krivanogov S.K. 1988. [Stratigraphy and paleogeography of lower Irtysh valley in the last glaciation (on carpological data)]. Nauka, Novosibirsk. [In Russian]
- Lacombat, F. 2005. Les rhinocéros fossiles des sites préhistoriques de l'Europe méditerranéenne et du Massif Central. *Paléontologie et implications biochronologiques*. BAR International Series, 1419:1-185.
- Lacombat, F. 2006. Morphological and biometrical differentiation of the teeth from Pleistocene species of *Stephanorhinus* (Mammalia, Perissodactyla, Rhinocerotidae) in Mediterranean Europe and the Massif Central, France. *Palaeontographica Abteilung A*, 274:71-111.
- Lobachev, Y.V., Vasiliev, S.K., and Orlova, L.A. 2012. Pozdnepleistocenovaya teriofauna s reki Chumysh (Altaisky krai) i novye dannye po mestonakhozdeniyu na reke Chik (Novosibirskaya oblast). *Problemy arkeologii, etnografii, antropologii Sibiri i sopredelnykh territoriy*, 18:106-110. [In Russian]
- Lobachev, Y.V., Lobachev, A.Y., and Billia, E.M.E. 2014. Morfologicheskie i biomekhanicheskie osobennosti zhevatelnogo apparata *Coelodonta antiquitatis* (Blumenbach, 1799) i *Stephanorhinus kirchbergensis* (Jäger, 1839), p. 168-170. In *Diversifikaciya i etapnost evolyucii organicheskogo mira v svete paleontologicheskoi letopisi*. Sankt-Peterburg. [In Russian]
- Martynov, V.A., Mizerov, B.V., Nikitin, V.P., and Shaevich, Y.E. 1977. Geomorphologicheskie struktury reki Ob okrestnostei Novosibirska. [In Russian]
- Mihlbachler, M.C. 2003. Demography of late Miocene rhinoceroses (*Teleoceras proterum* and *Aphelops malacorhinus*) from Florida: linking mortality and sociality in fossil assemblages. *Paleobiology*, 29:412-428. [https://doi.org/10.1666/0094-8373\(2003\)029%3C0412:dolmrt%3E2.0.co;2](https://doi.org/10.1666/0094-8373(2003)029%3C0412:dolmrt%3E2.0.co;2)
- Mihlbachler, M.C. 2005. Linking sexual dimorphism and sociality in rhinoceroses: insights from *Teleoceras proterum* and *Aphelops malacorhinus* from the late Miocene of Florida. *Bulletin of the Florida Museum of Natural History*, 45:495-520.
- Mihlbachler, M.C. 2007. Sexual dimorphism and mortality bias in a small Miocene North American rhino, *Menoceras arikareense*: insights into the coevolution of sexual dimorphism and sociality in rhinos. *Journal of Mammalian Evolution*, 14:217-238. <https://doi.org/10.1007/s10914-007-9048-4>
- Owen-Smith, R.N. 1975. The social ethology of the white rhinoceros *Ceratotherium simum* (Burchell, 1817). *Zeitschrift für Tierpsychologie*, 38:337-384. <https://doi.org/10.1111/j.1439-0310.1975.tb02010.x>
- Palmqvist, P., Gröcke, D.R., Arribas, A., and Fariña, R.A. 2003. Paleoeological reconstruction of a lower Pleistocene large mammal community using biogeochemical ( $\delta^{13}\text{C}$ ,  $\delta^{15}\text{N}$ ,  $\delta^{18}\text{O}$ , Sr:Zn) and ecomorphological approaches. *Paleobiology*, 29:205-229. <https://doi.org/10.1017/s0094837300018078>

- Panychev, V.A. 1979. Radiouglerodnaya chronologiya alluvialnykh otlozheniy Predaltayskoi ravniny. Nauka, Novosibirsk. [In Russian]
- Popowics, T.E. and Fortelius, M. 1997. On the cutting edge: tooth blade sharpness in herbivorous and faunivorous mammals. *Annales Zoologici Fennici*, 34:73-88.
- Pushkina, D., Bocherens, H., and Ziegler, R. 2014. Unexpected palaeoecological features of the Middle and Late Pleistocene large herbivores in southwestern Germany revealed by stable isotopic abundances in tooth enamel. *Quaternary International*, 339-340:164-178. <https://doi.org/10.1016/j.quaint.2013.12.033>
- Rusanov, G.G. and Orlova, L.A. 2013. Radiouglerodnye datirovki (SBRAS) Gornogo Altaya i Predaltayskoi ravniny. Biysk. [In Russian]
- Sanson, G. 2006. The biomechanics of browsing and grazing. *American Journal of Botany*, 93:1531-1545. <https://doi.org/10.3732/ajb.93.10.1531>
- Schaurte, W. 1966. Beiträge zur Kenntnis des Gebisses und Zahnbaues der afrikanischen Nashörner. *Säugetierkundliche Mitteilungen*, 14:327-341.
- Shpansky, A.V. and Billia, E.M.E. 2012. Records of *Stephanorhinus kirchbergensis* (Jäger, 1839) (Mammalia, Rhinocerotidae) from the Ob' River at Krasny Yar (Tomsk region, southeast of Western Siberia). *Russian Journal of Theriology*, 11:47-55.
- Shpansky, A.V. 2014. Juvenile remains of the "woolly rhinoceros" *Coelodonta antiquitatis* (Blumenbach 1799) (Mammalia, Rhinocerotidae) from the Tomsk Priob'e area (southeast Western Siberia). *Quaternary International*, 333:86-99. <https://doi.org/10.1016/j.quaint.2014.01.047>
- Shpansky A.V. 2016. New finds of Merck Rhinoceros (*Stephanorhinus kirchbergensis* Jäger 1839) (Rhinocerotidae, Mammalia) in Ob Area, Tomsk region. *Geosphere Research*, 1:24-39. [In Russian] <https://doi.org/10.17223/25421379/1/3>
- Shpansky, A.V., Svyatko, S.V., Reimer, P.J., and Titov, S.V. 2016. Finds of skeletons of *Bison priscus* Bojanus (Artiodactyla, Bovidae) from Western Siberia. *Russian Journal of Theriology*, 15:100-120. <https://doi.org/10.15298/rusjtheriol.15.2.04>
- Silaev, V.I., Ponomarev, D.V., Slepchenko, S.M., Bondarev, A.A., Kiseleva, D.V., Smoleva, I.V., and Khazov, A.F. 2015. Mineralogical and geochemical studies of bone detritus of Pleistocene mammals, including the earliest in Northern Eurasia Humans. *Bulletin of Perm University. Geology*, 4:6-31. <https://doi.org/10.17072/psu.geol.29.6>
- Steuer, P., Clauss, M., Südekum, K.-H., Hatt, J.-M., Silinski, S., Klomburg, S., Zimmermann, W., Fickel, J., Streich, W.J., and Hummel, J. 2010. Comparative investigations on digestion in grazing (*Ceratotherium simum*) and browsing (*Diceros bicornis*) rhinoceroses. *Comparative Biochemistry and Physiology. Part A: Molecular & Integrative Physiology*, 156:380-388. <https://doi.org/10.1016/j.cbpa.2010.03.006>
- Tong, H.W. and Wu, X.Z. 2010. *Stephanorhinus kirchbergensis* (Rhinocerotidae, Mammalia) from the Rhino Cave in Shennongjia, Hubei. *Chinese Science Bulletin*, 55:1157-1168. <https://doi.org/10.1007/s11434-010-0050-5>
- van Asperen, E.N. and Kahlke, R.-D. 2014. Dietary variation and overlap in Central and Northwest European *Stephanorhinus kirchbergensis* and *S. hemitoechus* (Rhinocerotidae, Mammalia) influenced by habitat diversity. *Quaternary Science Reviews*, 107:47-61. <https://doi.org/10.1016/j.quascirev.2014.10.001>
- Vasiliev, S.K. and Orlova, L.A. 2006. K voprosu o Taradanovskogo mestonakhozhdeniya fauny krupnykh mlekopitayushch. *Problemy arkheologii, etnografii, antropologii Sibiri i sopredelnykh territoriy*, 12(1):36-42. [In Russian]
- Vasiliev, S.K., Lobachev, Y.V., and Lobachev, A.Y. 2014. Novye dannye po mestonakhozhdeniyam pozdnepleistocenovoi megafauny na rekakh Chumysh i Chick (Altaiskiy kraj i Novosibirskaya oblast). *Problemy arkheologii, etnografii, antropologii Sibiri i sopredelnykh territoriy*, 15:15-18. [In Russian]
- Volkov, I.A. and Arhipov, S.A. 1978. Chetvertichnye otlozheniya raiona Novosibirska. Izdatelstvo IGI, Novosibirsk. [In Russian]
- Volkova, V.S. and Babushkin, A.E. (eds.) 2000. Uniphirovannaya stratigraficheskaya schema chetvertichnykh otlozheniy Zapadno-Sibirskoi ravniny. SNIIGMS, Novosibirsk. [In Russian]